RESULTS

3.1 DREAM complexes

It has recently been discovered that p130 and p107 are constituents of mammalian DREAM complexes. DREAM was first discovered in Drosophila embryonal cells and was named from its composition of Drosophila, Rb, E2F and Myb-interacting proteins (Lewis et al., 2004). Mammalian DREAM consists of a core DREAM (or LINC) complex comprised of Lin-9, Lin-37, Lin-52, Lin-54 and RBBP4 that associates with p130/E2F4 in G0/G1 to repress E2F-regulated genes or with B-Myb in S/G2 to activate genes required for mitosis (Figure 3.1). The p107 pocket protein can act redundantly with p130 to form repressive E2F4/LINC complexes, particularly in situations where p130 is scarce or absent.

One of the main aims of this study was to identify the presence or absence of repressor DREAM complex with regards to p130/E2F4, the G0/G1 DREAM complex in HPV-transformed cell lines. It is established that E7 interacts with pRB by its LXCXE motif but we are still unclear whether the E7 will disrupt the p130/DREAM complex binding towards E2F4 transcription factor during the G0/G1 in cell cycle. It is noted that a Drosophila DREAM-like complex (Myb-E2F2/RBF) is resistant to dissociation by Cdk-phosphorylation (Lewis *et al*., 2006), although this modification is well known to disrupt other pocket protein/E2F complexes. It is possible, therefore, that DREAM complexes are relatively resistant to dissociation. Indeed, p130 and p107 were both found to be present in DREAM complexes in HeLa cervical carcinoma cells, suggesting that HPV18 E7 expression is insufficient to dissociate these complexes (Pilkinton *et al*., 2007). On the other hand, it has been found that E7 encoded by both high-risk and low-risk HPV types is able to cause degradation of p130 (Zhang *et al*.,

2006). In order to investigate the effect of E7 towards p130/DREAM complex, four types of cell lines were employed in this study.

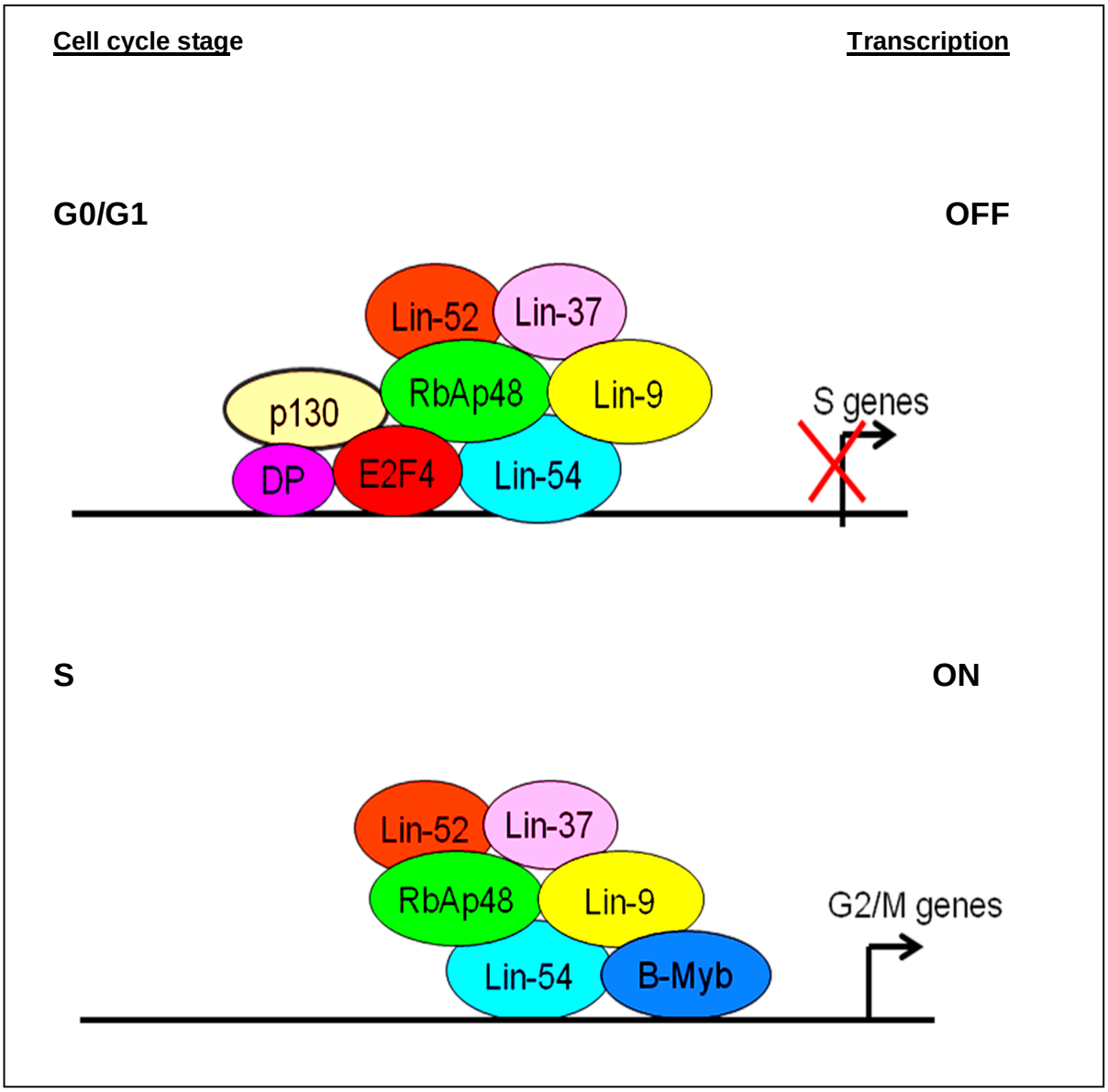

Figure 3.1: DREAM complexes constituents (Lin52, Lin37, Lin9, Lin54, RbAp48) interacting with pocket protein (p130), E2F4 transcription factor and DP and cell cycle transactivator gene (B-myb). In quiescent cells (G0/GI), DREAM complexes associates with E2F4/p130 to repress E2F- regulated genes. During cell cycle entry, E2F4 and p130 dissociate and DREAM complexes associate with B-myb to activate genes required for mitosis.

3.1.1 Analysis of DREAM complexes in T98G, C33A, SiHa and CaSki cell lines.

Experiments were performed to determine whether the expression of E7 resulted in loss of specific DREAM complexes. To correlate the disruption or presence of DREAM complexes with the expression of HPV16 E7 protein, four cell lines (T98G, C33A, SiHa and Caski) have been employed. T98G glioblastoma cells were used as a control, since the DREAM complexes have been well-characterised in this cell line**.** C33A is a cervical carcinoma cell line which does not carry any HPV genes, whereas SiHa and Caski cells are HPV16 positive with 2 copies and 600 copies of the E7 gene per cell, respectively. In these experiments, the core DREAM component (Figure 3.1) was immunoprecipitated using Lin9 antibodies. Nuclear lysates from all four cells were immunoprecipitated with pre-immune rabbit serum (control) and Lin9 antibody and western blotted with B-myb, p107, p130 and Lin-9. Ten percent of total lysate from each cell was retained and immunoblotted as an input control.

It was evident from the resulting immunoblots that expression of p130 is much more abundant in the control T98G and C33A cell lines as compared to SiHa and Caski cell lines expressing 16E7, as indicated by the relative intensities of input control bands (Figure 3.2). The reduced p130 levels in SiHa and Caski cells is presumably due to E7-mediated degradation (Roman *et al*.,2006). Furthermore, immunoprecipitation with anti-Lin9 antibody demonstrated that p130/DREAM complexes are most abundant in T98G cells (Figure 3.2) and scarce in 16E7-expressing cells (in particular Caski), and this presumably reflects both the reduced p130 levels as well as interference with binding of p130 to E2F4 by 16E7. Expression of p107 is relatively low compared to p130 in all cell lines, and p107 is at most a

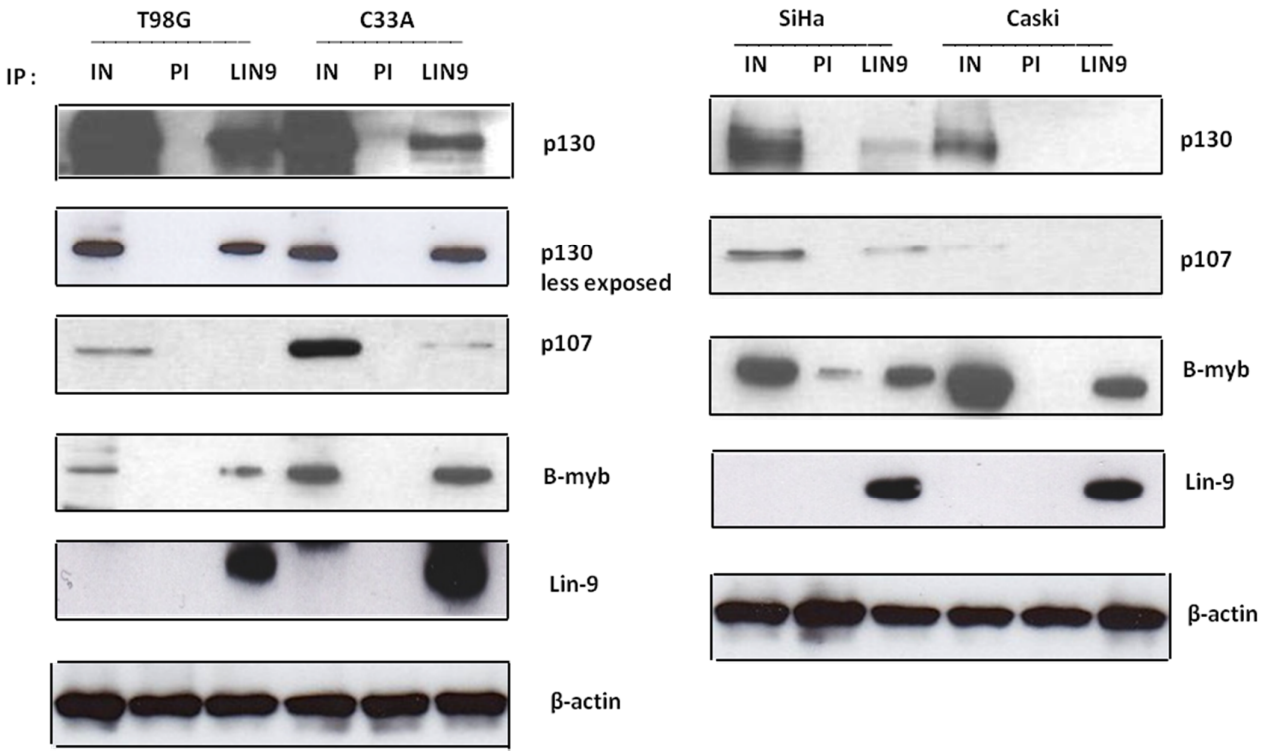

Figure 3.2: Identification of DREAM complexes in T98G, C33A, SiHa and Caski cell lines. DREAM complexes were immunoprecipitated from nuclear lysates of the HPV-negative cell lines T98G and C33A and the HPV16-positive cell lines SiHa and CaSki with control pre-immune serum (PI) or Lin-9 antibody. lmmunoprecipitates (IP) were blotted for p130, p107, B-myb and Lin-9 proteins. All protein samples were run in parallel and blots were exposed equally to film, except for the lesser exposure of the pl30 blot of T98G and C33A lysates. The input control (IN) comprised 10 % of the lysates used for immunoprecipitation. Ten per cent of the lysates remaining after immunoprecipitation were also run against an input control and probed with β-actin antibody as a check for loading.

minor constituent of DREAM complexes. However, it is notable that p107 expression was increased in C33A cells as indicated from the input control (Figure 3.2). Moreover, minor p107/DREAM complexes were detected in C33A and SiHa cell lines but were completely absent from Caski cells (Figure 3.2).

B-myb expression, as indicated by the input controls, was higher in SiHa and Caski cells compared to the control cell lines. This is likely the result of deregulation of B-myb expression by HPV16 E7. It is also apparent, that B-myb was co-precipitated with Lin-9 in all cell lines but the level of B-myb/Lin-9 was much higher in the 16E7-expressing cell lines, SiHa and Caski (Figure 3.2). This presumably results from increased B-myb expression and additionally disruption of competing p130/DREAM complexes.

Therefore, expression of 16E7 correlates with increased expression of B-myb/Lin-9 and concomitant decreased expression of p130/Lin-9, especially in Caski cells (containing 600 copies of the E7 gene). All blots were blotted against Lin-9 antibody in this experiment as a control for the Lin-9 immunoprecipitation (IP) (Figure 3.2). However, as found in some previous studies (Osterloh et al., 2007), Lin-9 could not be detected in input controls but only when first immunoprecipitated the Lin-9 antibody..

3.2. Interference of 16E7 RNA in HPV-transformed cell lines.

3.2.1 Effects of 16E7 depletion on pocket protein/DREAM complexes in Caski and SiHa cells

To confirm that disruption of pocket protein/DREAM complexes in Caski and SiHa cells was dependent on HPV16 oncoprotein expression, the RNA interference approach was used. Therefore we knocked down E7 expression in SiHa and Caski cells with lentivirus vectors (pLKO.1 puro) carrying 16E7 shRNA genes. To overcome the transfection efficiency problems encountered in preliminary experiments the shRNA vectors were packaged into lentiviral particles. The 16E7 shRNAs used in this study, were selected from two published papers (Sima *et al*, 2008 and Rampias *et al*, 2009) and named as 16E7A and 16E7B, respectively. These 16E7 shRNAs were chosen because they showed a high percentage of E7 knock down in Caski cells. Control cells were transduced with a lentivirus vector expressing a scrambled shRNA. The transductions were performed in SiHa and Caski cells and the transfected cells were selected with puromycin 24 hours post transduction. The cells were harvested after 48 hours of puromycin selection.

As shown in Figure 3.3a, the transduction of Caski cells with 16E7-shRNAs resulted in a significant decrease in mRNA expression of E7 oncogene. After transduction, the amount of E7 mRNA in Caski cells transduced with 16E7A and 16E7B shRNAs decreased by 64% and 96.8% respectively compared with cells receiving scrambled control shRNA. Similarly, in SiHa cells the E7 mRNA expression was decreased by 72% and 98.8% with 16E7A and 16E7B shRNAs, respectively (Figure 3.3b). To analyse the cell cycle progression in SiHa and Caski cells following E7 knock-down, FACS analysis was performed. The results show that cells accumulated at G1 in 16E7- depleted Caski cells, with 79.3% and 83.5% G1 cells

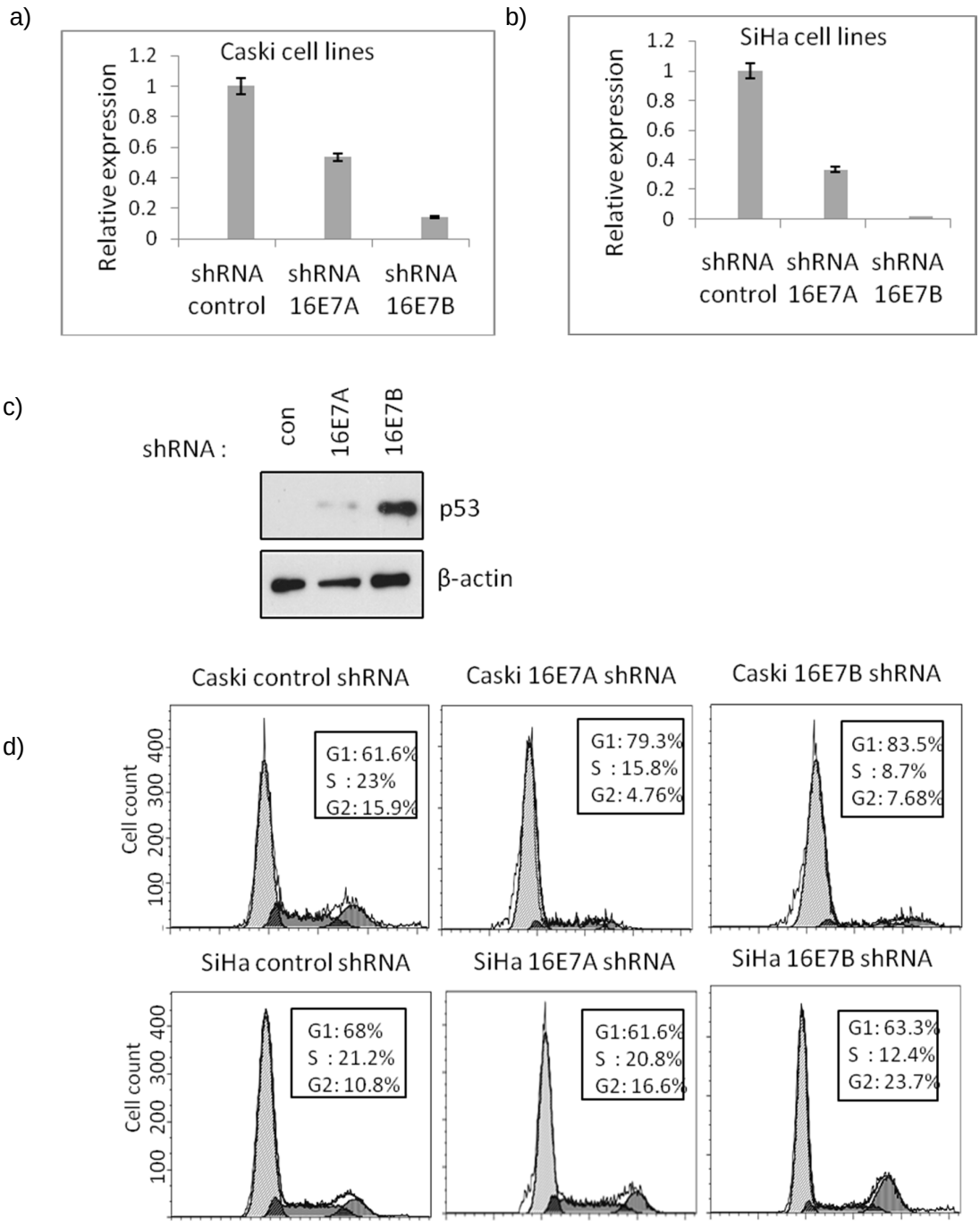

Figure 3.3: Depletion of E7 in SiHa and Caski cells. Quantitative PCR (qPCR) analysis of E7 RNA expression in (a) Caski and (b) SiHa E7-depleted cells relative to control cells. Expression was normalized to ribosomal *ARP PO*. Flow cytometry (FACS) analyses of E7-depleted in (c) Caski control (scrambled shRNA), Caski 16E7A and Caski 16E7B and (d) SiHa control (scrambled shRNA), SiHa 16E7A and SiHa 16E7B stained with propidium iodide (PI)

induced by 16E7A and 16E7B shRNA respectively, compared to 61.6% in control cells (Figure 3.3d). These results are consistent with previously published studies, which also showed a profound G1-arrest upon E7 knockdown (Tang *et al*., 2006). Interestingly, the S phase cells decreased significantly in E7-depleted Caski cells with only 15.8% and 8.7% at this cell cycle phase in cells transduced with 16E7A and 16E7B shRNAs, compared to control cells with 23% cells in S phase. These results clearly demonstrated that the cell cycle was arrested at G1 when 16E7 was suppressed in Caski cells, however, a different effect was found in SiHa cells. E7-depleted SiHa cells did not accumulate significantly in G1, however there was an obvious increase in the proportion of G2/M phase cells (Figure 3.3d), particularly in SiHa cells transduced with 16E7B shRNA (23.7% compared to 10.8% with the control shRNA).

To investigate whether the impact of E7 suppression on the cell cycle in Caski was reflected in effects on pocket protein/DREAM complex association, nuclear lysates from shRNA-transduced cells were immunoprecipitated with Lin9 antisera and western blotted against B-myb, p130 and Lin-9. The results demonstrated that expression of B-myb was reduced in Caski cells transduced with 16E7A shRNA and completely lost by transduction with 16E7B shRNA (Figure 3.4). As shown by the flow cytometry analyses, 16E7 shRNA tranduction decreased significantly the proportion of Caski cells in S phase, and this is reflected in the down-regulation of B-myb expression when the E7 was depleted. In contrast, the p130/DREAM complexes were reformed in Caski cells transduced by 16E7B shRNA, accounting for the G1 cell cycle arrest. The reformation of the p130/DREAM complex was presumably due to removal of 16E7 that otherwise would bind to p130 and directly block its association with E2F4-DREAM. In addition, p21 and p27 may become active upon 16E7 depletion to suppress cyclin E/A-CDK2 phosphorylation of p130 during S phase. As an IP control, all blots were blotted against Lin-9 antibody (Figure 3.4).

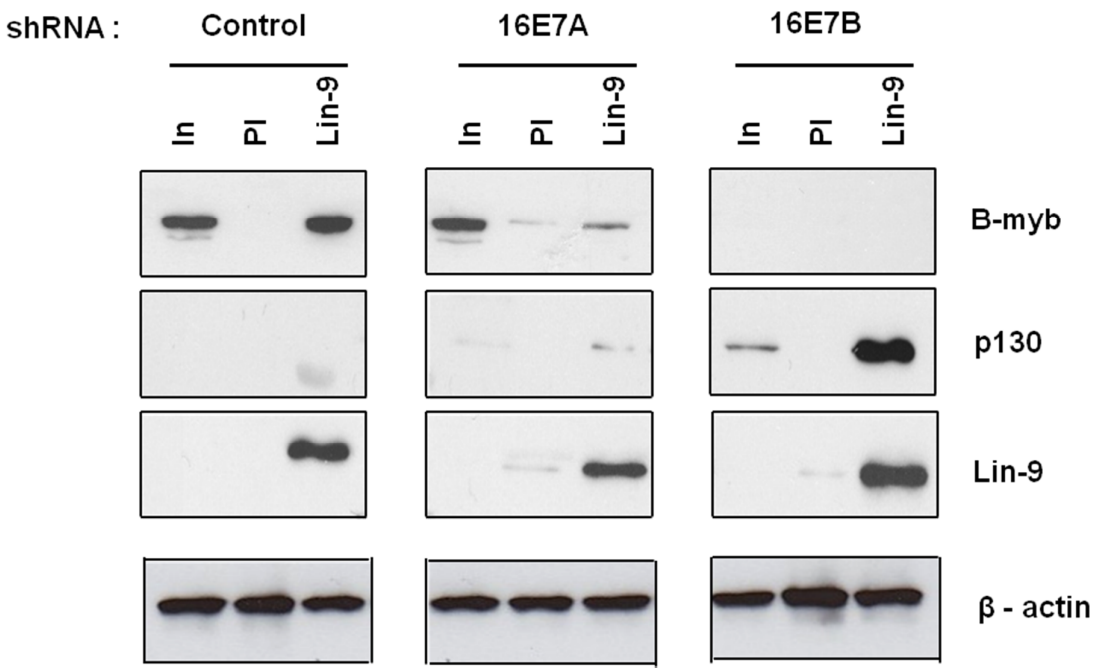

Figure 3.4: Immunoblot of DREAM complexes in Caski E7-depleted cells. Caski cells were transduced with Lentiviral scrambled (control), 16E7A and 16E7B. Western blotting was performed on the transfected nuclear lysates against B-myb, p130 and Lin-9. The input control (IN) comprised 10% of the lysates and the pre-immune (PI) serum was used as a control for immunoprecipitation (IP). Proteins were separated in 10% SDS-PAGE and western blotted onto a nitrocellulose membrane. All blots were equally exposed to film at 20 minutes.

Caski cells contain integrated HPV16 E6 and E7 oncogenes at 600 copies per cell. Since E6 targets p53 for degradation, Caski cells will also lack p53 expression, which is an important tumour suppressor gene besides pRB. It is also known that suppressing the E7 gene by RNA interference will inevitably knock-down E6 expression as well, as mRNAs encoding these proteins are bicistronic. To determine the effect of the shRNAs on p53 expression, a western blot was performed. As expected, the p53 expression was increased upon E7 suppression in Caski cells (Figure 3.3c). Notably, 16E7B shRNA had a more profound effect upon p53 induction.

To determine whether G1 arrest precipitated by E6/E7 knockdown in Caski cells is dependent on DREAM complex reformation, we tested whether depleting expression of one of the core DREAM complex components, Lin-54, could overcome the effect of E7 depletion on the cell cycle. A number of lentivirus vectors expressing Lin54 shRNAs were assessed by qPCR and the most effective in depleting Lin54 mRNA expression was used in the analysis. As a further test for Lin54 depletion, DREAM complexes were immunoprecipitated using Lin54 antibody from Caski cells transduced with the Lin54 and control shRNA vectors and tested for co-immunoprecipitation of B-Myb. This assay was performed as Lin54 itself is difficult to detect by western blotting, whereas B-Myb is expressed at high levels in cells carrying 16E7 proteins. The results showed that Lin-54 expression was efficiently suppressed in Caski cells when compared to the control cells (Figure 3.5a). Subsequently, the Lin-54 shRNA was co-transduced with the 16E7B shRNA in Caski cells and cells were harvested for cell cycle analysis by propidium iodide staining and flow cytometry. This showed that whereas 83.5% of 16E7B shRNA transduced cells were in G1, this was reduced to 56.8% when Lin54 shRNA was co-transduced with 16E7B shRNA (Figure 3.5c). There was also a pronounced increase in S phase cells in the Lin54 shRNA co-

transduced cells compared to cells transduced with 16E7B shRNA alone (18.8% compared to 8.7%, respectively). The results then clearly demonstrate the requirement for Lin54, and by extension the DREAM complex, for G1 arrest in Caski cells depleted for E6/E7 expression.

To confirm that reformation of p130/DREAM is important for G1 arrest upon E6/E7 depletion, CaSki cells were transduced with 16E7B shRNA either alone or together with p130 shRNA. Flow cytometry showed that co-transduction of p130 shRNA strongly overcame the G1 arrest caused by 16E7B shRNA (Figure 3.6). In addition, qPCR analysis showed an increase in expression of B-myb and cyclin A, which are transcriptionally repressed by p130/DREAM (Litovchick et al., 2007), upon co-transduction of 16E7B shRNA expressing cells with p130 shRNA (Figure 3.6).

Figure 3.5 : G1 arrest induced by E7 depletion in Caski cells is Lin54-dependent. (a) Nuclear lysates from untransduced CaSki cells (CaSki) or CaSki cells transduced with lentiviruses encoding control or Lin-54 shRNAs were immunoprecipitated with pre-immune serum (PI) or Lin-54 antibodies and blotted for B-myb. The input (In) control comprised 10% of the lysates used for immunoprecipitation. (b) Detection of p130 in immunoprecipitates of CaSki cells transducted with lentiviruses encoding control shRNA, 16E7B shRNA and a combination of 16E7B and Lin-54 shRNAs. Pre-immune serum (PI) and Lin-9 antibodies were used for immunoprecipitation and p130 was detected on Western blots. The input (In) control comprised 10% of the lysates used for immunoprecipitation. (c) Flow cytometry of propidium iodide-stained CaSki cells transduced with lentiviruses encoding control shRNA, 16E7B shRNA and a combination of 16E7B and Lin-54 shRNAs. The estimated percentages of cells in G1, S and G2/M phases are shown.

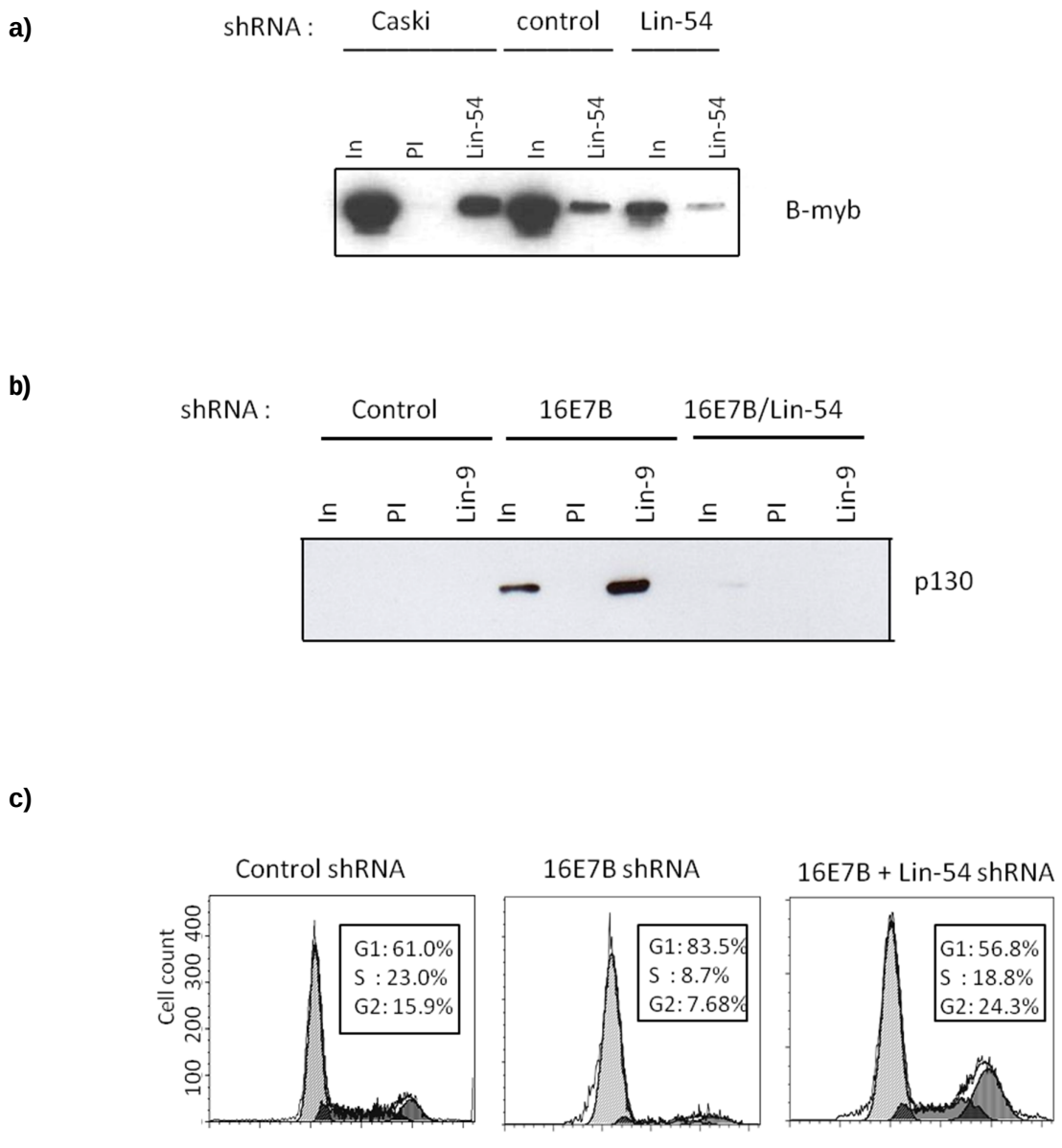
a)
shRNA :
Caski
control
Lin-54
In
PI
Lin-54
In
Lin-54
In
Lin-54
B-myb
b)
shRNA :
Control
16E7B
16E7B/Lin-54
In
PI
Lin-9
In
PI
Lin-9
In
PI
Lin-9
p130
c)
Control shRNA
16E7B shRNA
16E7B + Lin-54 shRNA
Cell count
100
200
300
400
G1: 61.0%
S : 23.0%
G2: 15.9%
G1: 83.5%
S : 8.7%
G2: 7.68%
G1: 56.8%
S : 18.8%
G2: 24.3%

Figure 3.5

Figure 3.6: G1 arrest induced by E7 depletion in Caski cells is p130-dependent. (a) Quantitative PCR (qPCR) analysis of p130 RNA expression in CaSki p130-depleted cells relative to control cells. Expression was normalised to ribosomal *ARP PO*. (b) Flow cytometry (FACS) analysis of propidium iodide- stained CaSki cells transduced with lentiviruses encoding control shRNA, 16E7B shRNA and a combination of 16E7B and p130 shRNA. The estimated percentages of cells in G1, S and G2/M phases are shown. (c) Quantitative PCR (qPCR) analysis of B-myb and cyclin A RNA expression in CaSki cells transduced with lentiviruses encoding 16E7B shRNA and a combination of 16E7B and p130 shRNA. Expression was normalised to ribosomal *ARP PO*.

a)

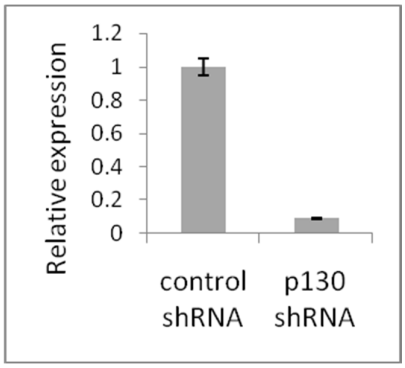

b)

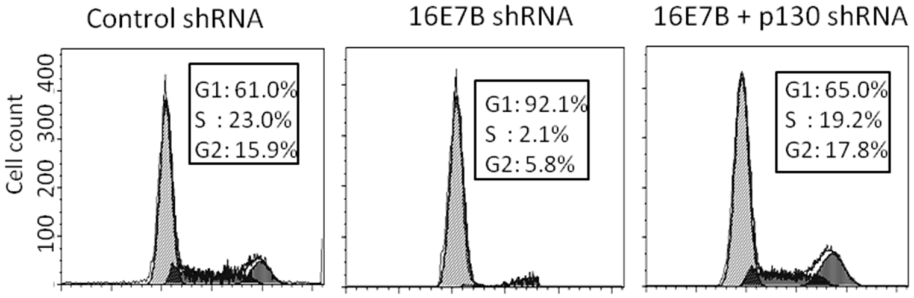

c)

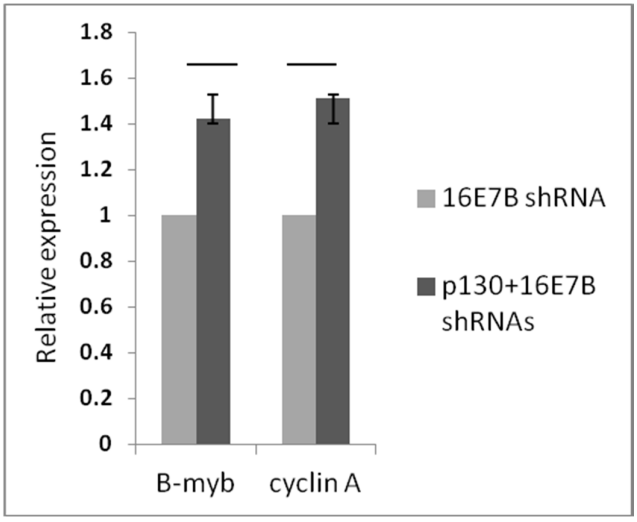

Figure 3.6

3.3 Disruption of pocket protein/DREAM complexes by different HPV E7 types.

The ability of the high risk HPV16 E7 protein to bind pRB, p107 and p130 is well established (Davies *et al.*, 1993). E7 proteins from the low risk HPV types generally bind to the retinoblastoma tumor suppressor family with lower affinity than those expressed by high risk types. In order to establish a rigorous assay for the effects of various E7 proteins on DREAM complexes, E7 proteins from a number of different HPV types were expressed ectopically in T98G cells, which have well characterized DREAM complexes. Six different E7 proteins were assayed in this system, from the high risk types HPV16, HPV18 and HPV33, the low risk type HPV11 and the cutaneous types HPV1 and HPV48 (Table 3.1). T98G cells were transiently transfected with HA-tagged E7 genes cloned in the pMSCVpuro vector using the calcium phosphate co-precipitation method. Transfected cells expressing the E7 types were selected with puromycin. To test whether the E7 proteins were expressed at comparable levels, 100 μg of nuclear lysates were immunoprecipitated with HA antibody, resolved in a 15% SDS-PAGE gel and western blotted with an anti-HA mouse monoclonal antibody. It was found to be necessary to western blot the E7 proteins onto a PVDF membrane, as the low expression levels made them more difficult to detect on a nitrocellulose membrane. The resultant western blot (Figure 3.7) showed expression of each E7 type at comparable levels, albeit with some minor variation.

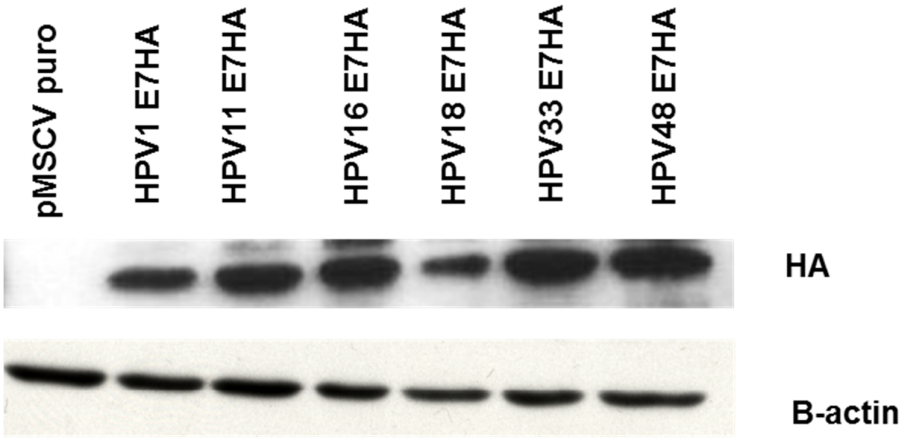

Figure 3.7: Ectopic expression of various HPV E7 types in T98G cells. 30 µg of each pMSCVpuro-E7-HA construct and the pMSCVpuro vector control were calcium phosphate transfected for transient expression in T98G cells. Transfected cells were puromycin selected and nuclear lysates were harvested 48 hours post transfection. Nuclear lysates were immunoprecipitated with HA antibody, separated on a 15% SDS-PAGE gel and western blotted onto a PVDF membrane. E7 proteins were detected using HA antibody.

HPV type	LXCXE motif	Pocket protein binding	Pathogenicity
1	L Y C Y E	High affinity	Plantar warts
11	L H C Y E	Low affinity	Genital warts
16	L Y C Y E	High affinity	Intraepithelial neoplasias & carcinoma
18	L L C H E	High affinity	Intraepithelial neoplasias & carcinoma
33	L Y C Y E	High affinity	Intraepithelial neoplasias & carcinoma
48	L I S D E	No binding	Non melanoma carcinomas

Table 3.1: The integrity of the LXCXE motif, pocket protein affinity and pathogenicity of each HPV employed in this study. HPV types that have frequently been associated with malignant progression are underlined. The L, C and E residues present within the putative LXCXE motif of each HPV type are shown in red. It is important to note that the classification of each E7 type as having low or high pocket protein affinity is a broad categorisation. Each E7 type binds to the pocket proteins with a different affinity. Information was taken from Munger et al., 1989; Ciccolini et al., 1994; Caldeira et al., 2000; Dong et al., 2001)

In vitro studies performed previously (Pearce., 2007, PhD thesis) showed that 16E7 could disrupt pRB/Lin-9 binding at a significantly lower input than with the other E7 types. To determine whether this correlation would also apply to pocket protein/DREAM complex disruption, nuclear lysates from T98G cells transfected with the various E7s were assessed by immunoprecipitation with Lin-9 antibody and blotting against p130, p107 and B-myb. The results obtained with the input controls indicated that expression of p130 was reduced in cells expressing high risk 16E7, 18E7, 33E7 and low risk 11E7, which is probably due to E7-mediated degradation (Roman *et al.*,2006) (Figure 3.8). This is also reflected in the p130/DREAM complexes, which were greatly disrupted by 16E7, 18E7 and 33E7 because they can bind to pocket proteins at high efficiency and thereby disrupted the interaction with the DREAM complex (Tommasino and Crawford, 1995). Even though 11E7 reduced p130 expression, it did not reduce p130/DREAM complex formation to the same extent as the high risk E7 proteins (Figure 3.8), which is related to its lower efficiency binding to pocket proteins (Munger K *et al.*,1989). On the other hand, expression of 1E7 from a cutaneous HPV type did not decrease p130 levels to the same extent, as indicated by the input control. However, it did result in diminished p130/DREAM complex formation compared to control cells, presumably by interfering with binding of p130 to E2F4, as it has the same affinity as 16E7 for binding to pocket proteins (Ciccolini *et al.*, 1994). The results obtained with 48E7, which is encoded by another cutaneous HPV type and lacks a LXCXE motif, were quite unexpected, as it slightly reduced the p130 levels and significantly disrupted the p130/DREAM complex even though 48E7 binds to pocket proteins with extremely low affinity (Caldeira *et al.*,2000; Dong *et al.*,2002). However, (Pearce J,2007;Ph.D thesis) has shown that 48E7 protein was competent to bind to the Cdki p21 *in vitro*. It is known that p21 is involved in E2F/pocket protein-cyclinE/A-CDK2 pathways in G1 and

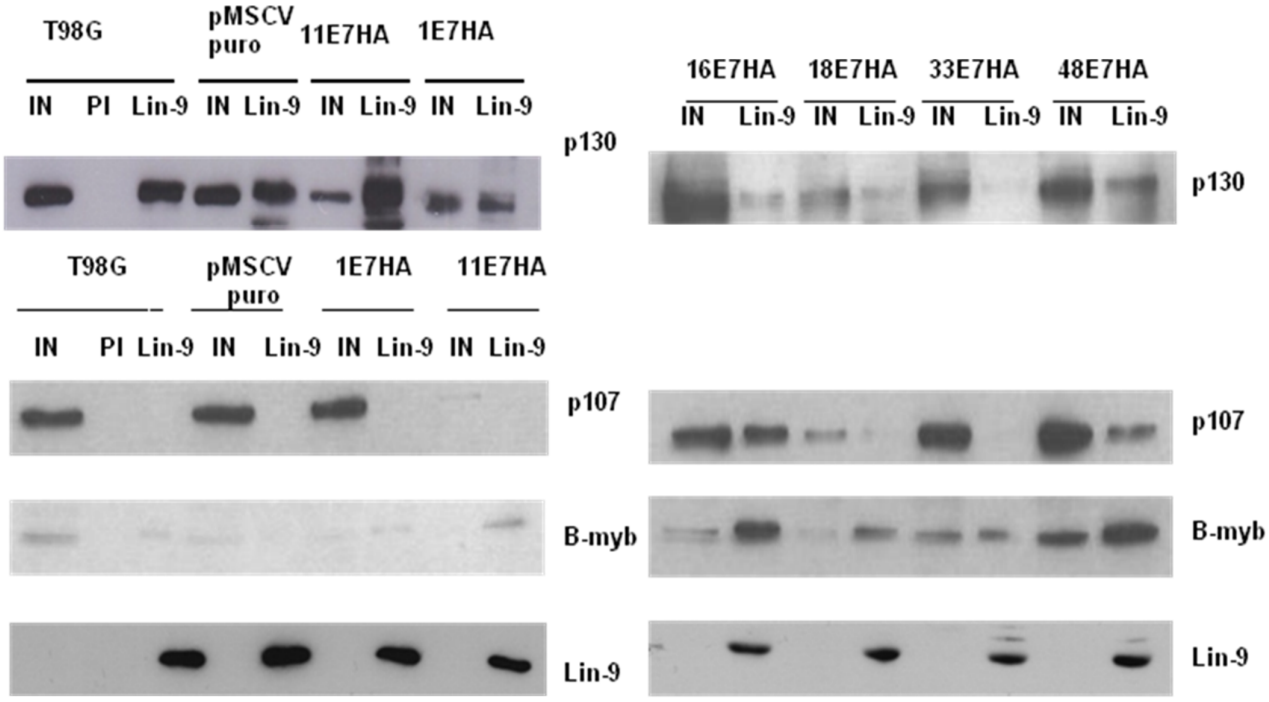

Figure 3.8: Immunoblot of DREAM complexes in T98G cells expressing various HPVE7 types. 30 μg of pMSCV puro vector and this vector encoding 11E7-HA, 1E7-HA, 16E7-HA, 18E7-HA, 33E7-HA and 48E7-HA were calcium phosphate transfected for transient expression in T98G cells. Transfected cells were puromycin selected and nuclear lysates were harvested at 48 hours post transfection. Immunoprecipitations were performed on nuclear extracts using Lin-9 antiserum and proteins were separated in 10% SDS-PAGE gels. Western blots were then probed for p130, p107, B-myb and Lin-9. All blots were equally exposed to film at 15 minutes.

S phase. By binding to p21, 48E7 will abrogate its inhibition of cyclin/CDK activity and therefore lead to p130 hyperphosphorylation. This is predicted to result in impairment of p130-DREAM complex formation and may also affect p130 stability.

Expression of p107 is usually low when compared to p130 in T98G cells and p107 is a minor constituent of DREAM complexes. However, p107 expression is induced following the G1/S transition. There was no detection of the p107/DREAM complex in T98G cells transfected with the control vector or in cells transfected with most E7 types, however, p107/DREAM was detectable in cells transfected with 16E7 and 48E7 (Figure 3.8). The formation of p107/DREAM complexes upon 16E7 and 48E7 expression presumably reflects their ability to disrupt the p130/DREAM complex (Figure 3.8), either through direct interaction of 16E7 with p130 or possible effects of both 16E7 and 48E7 on Cdk2 phosphorylation activity and promotion of the cell cycle into S phase entry. It is notable that 16E7 and 48E7 expression also induced the most pronounced increase on B-myb/DREAM complex formation (Figure 3.8). Whereas 18E7, 33E7 and to a lesser extent 11E7 also induced this complex to an extent, when compared to the non-transfected cells and vector only control (Figure 3.8), 16E7 and 48E7 induced equivalently the highest B-myb/DREAM complex expression. Schmit *et al.*,2007, have demonstrated that p107 associates with the B-myb/DREAM complex in T98G cells, and the presence of p107 in DREAM complexes in HPV16 E7 and HPV48 E7 transfected cells may therefore relate to this association rather than the formation of repressive complexes.

These results demonstrate that both high risk and low risk HPV E7 protein have the ability to dissociate pocket protein/DREAM complexes, even though the low risk HPVE7 types bind at lesser affinity to the pocket proteins. Studies on the E7 proteins from low risk HPV types 6 and 11, which are rarely associated with malignant lesion, have demonstrated that a reduced affinity for pRB correlates with a lack of in vitro

transforming activity (Storey *et al*., 1988; Munger *et al*., 1989). However, strong affinity does not necessarily correlate with the ability to induce cellular transformation (Caldeira *et al*, 2000). Indeed, the E7 protein from the low risk HPV type 1 can associate strongly with pRB, but fails to induce degradation and transformation (Alunni-Fabbroni *et al*., 2000).

3.4 Human papillomaviruses disrupt p130/DREAM complexes through different mechanisms.

3.4.1 Identification of DREAM complex in CaSki expressing various types p130 mutants.

The results obtained so far suggest that E7 must target p130 for HPV16 to promote the host cell to exit from quiescence (G0) state and enter S phase. Thus, the results showed that p130/DREAM complexes were reformed in 16E7-depleted cells and caused a profound cell cycle arrest at G1 phase. It was also shown that both p130 and DREAM are essential for this cell cycle arrest. These findings provide a molecular mechanism which adds to previous observations showing that p130 is the most important target for HPV E7 oncoproteins during the normal replication cycle to promote the keratinocytes into S phase (Genovese et al., 2008), a state which is conducive for the early stages of viral replication. E7 proteins could potentially target the p130/DREAM complex through two known mechanisms: direct interaction with p130 or induction of CDK2 phosphorylation via an interaction with p21. To explore which of these mechanisms are responsible for the activities of 16E7 and 48E7 on disruption of p130/DREAM and cell cycle progression, p130 mutants were used (Figure 3.9).

Therefore, further experiments were conducted with a p130 mutant that is defective in binding the E7 LXCXE motif (p130mE7) and another mutant which cannot be phosphorylated by CDK (p130PM22). In addition, a double mutant (p130PM22/mE7) was constructed. The p130mE7 mutant was designed based on the work of Dick and Dyson (2002), who showed that a surface of the pRB B pocket was critical for binding LXCXE motif-containing proteins including HPV 18E7. This region

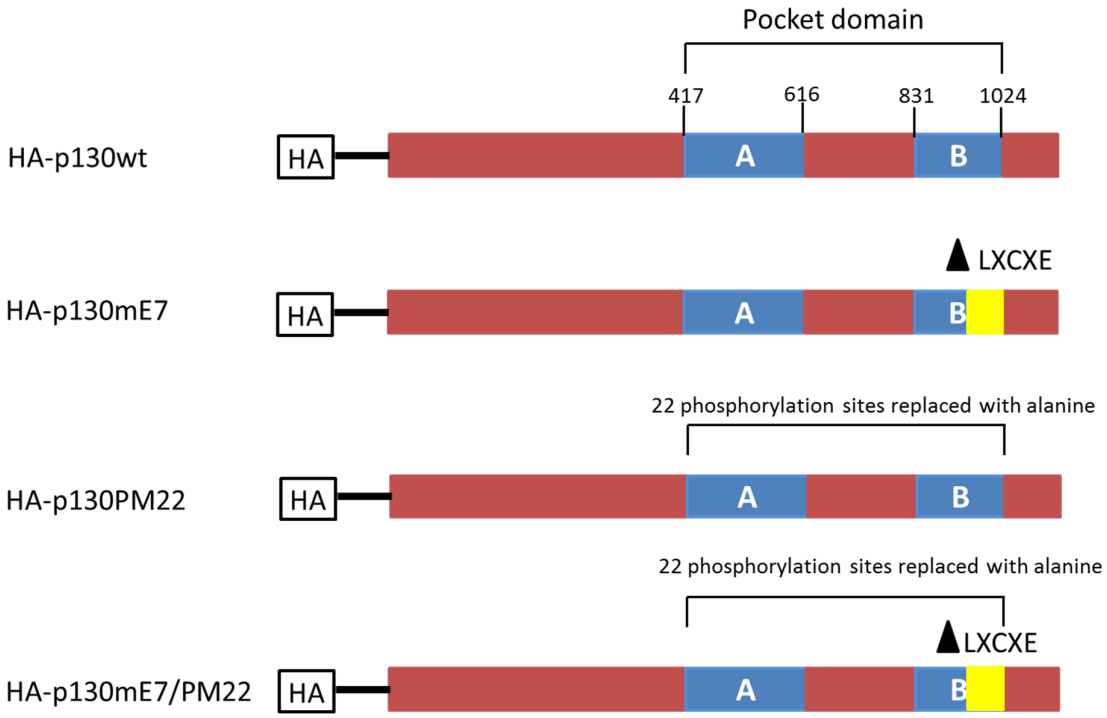

Figure 3.9: Schematic summary of the constructed p130 mutants based on the p130wt. p130wt has two pocket domains which are A and B for viral oncoproteins binding and cyclin dependent kinase phosphorylation. P130mE7 was designed by replacing serine and threonine in B pocket with alanine. In p130PM22, 22 phosphorylation sites of serine and threonine were mutated with alanine. In addition, p130PM22/mE7 was mutated for CDK phosphorylation and E7 binding sites at the LXCXE motif on B pocket of p130.

of the pRB B pocket is partially conserved in p130, and two critical conserved amino acids (leucine and cystine) in p130 were replaced with alanine by *in vitro* mutagenesis. Zi Ling, our undergraduate student has shown that p130mE7 is unable to bind E7 by GST fusion binding assay (Figure 3.10). The p130PM22 mutant has been mutated at the 22 CDK phosphorylation sites by replacing the phosphorylated serine and threonines with alanine (Farkas et al., 2002). The p130PM22/mE7 protein was mutated at both the E7 binding and phosphorylation sites. All p130 mutants and a control wild-type p130 were tagged with HA to differentiate between endogenous and ectopically expressed p130.

Firstly, expression of the HA-tagged p130 proteins were compared in C33a and CaSki cells by transfecting these plasmids in Fugene 6 transfection reagent. The transfected cells were harvested and immunoblotted using p130 and HA antibodies. It was found that all p130 mutants were equally expressed in the HPV-negative C33a cells, as none of the p130 proteins could be targeted by E7 in this cell line (Figure 3.11). In contrast, neither p130 wt nor p130PM22 were expressed in CaSki cells, whereas the p130mE7 and p130PM22/mE7 mutants were both detectable on the HA antibody blot (Figure 3.11). This finding strongly suggested that the p130mE7 mutation prevented binding to 16E7 in Caski cells and thus protected it from degradation. On the other hand, CDK phosphorylation of p130 did not appear to be a major factor in degradation of this protein in Caski cells, as the p130PM22 mutant was not protected. Immunoblotting with the p130 antibody did not show increased expression of p130 in the transfected cells, suggesting that the HA-tagged wild-type p130 and the mutants were expressed at a relatively low level, compared to endogenous p130.

To determine whether the p130mE7 and p130PM22/mE7 mutants could complex with DREAM in CaSki cells, the nuclear lysates from transfected cells were co-precipitated with Lin-9 and probed on western blots using HA antibody. As

a)

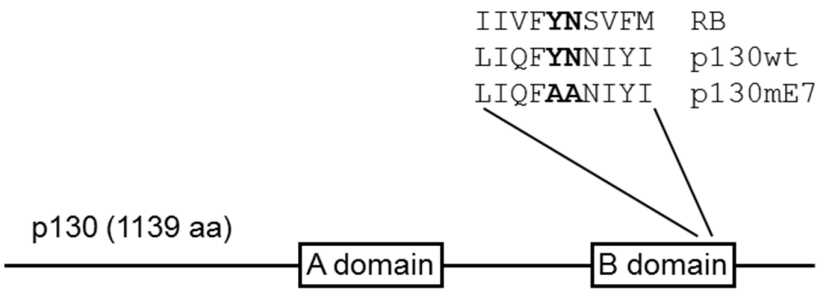

b)

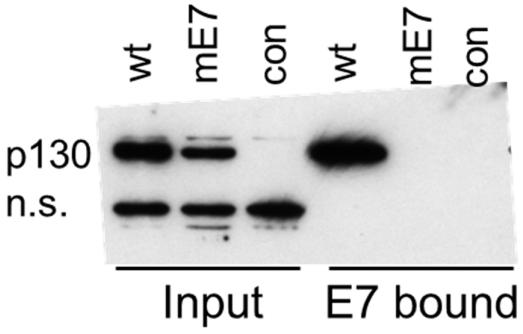

Figure 3.10: The p130mE7 mutant is unable to bind 16E7. (A) Schematic of the 1139 amino acid human p130 protein, showing the A and B domains of the pocket. Also indicated is the region of the B domain conserved between RB and p130 which was mutated in p130mE7. In p130mE7, amino acids Y1009 and N1010 were changed to alanines. (B) Nuclear extracts were prepared from T98G cells transfected with the pMSCVpuro vector encoding HA-tagged p130wt or p130mE7 and from cells transfected with the empty vector (con). Nuclear extracts (150 μg) were incubated with 20 μg 16E7 protein bound to glutathione-Sepharose beads and the selected proteins were eluted and analysed by western blot alongside inputs comprising 15 μg of each nuclear extract. The p130wt and p130mE7 were detected using an HA antibody probe. In addition to the p130 proteins, a non-specific (n.s.) band was seen with the input samples. (Adapted from Zi Ling, masters thesis)

Figure 3.11: Expression of various p130 mutants in C33a and CaSki cell lines.

pMSCV puro constructed with p130 wt and p130 mutants (p130mE7, p130PM22 and p130 mE7/PM22) were 'FuGENE 6' transfected in C33a and CaSki cells. Transfected cells were puromycin selected and nuclear lysates were harvested 48 hours post transfection. Nuclear lysates were separated on a 10% SDS-PAGE gel and western blotted onto a nitrocellulose membrane. Endogenous and ectopically expressed p130 were detected by p130 and HA antibodies, respectively. B-actin was used as a loading control.

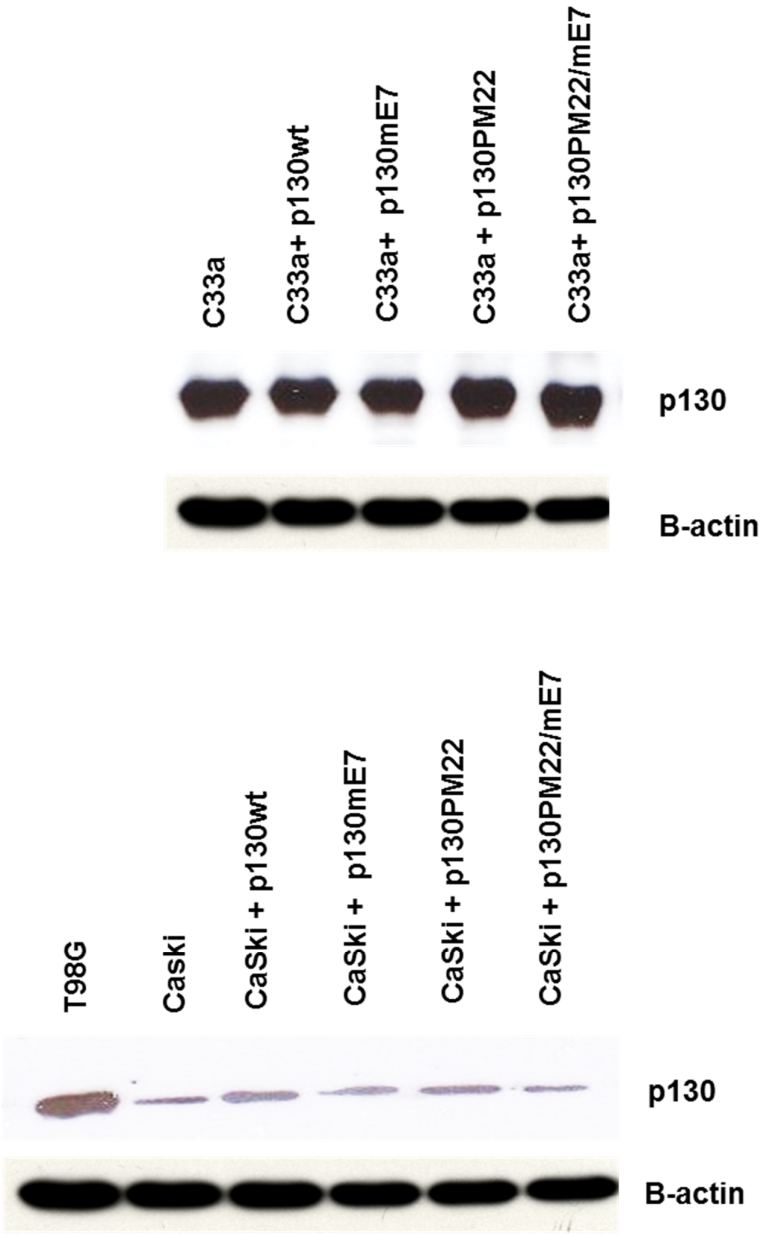
C33a
C33a+ p130wt
C33a+ p130mE7
C33a + p130PM22
C33a+ p130PM22/mE7
p130
B-actin
T98G
Caski
CaSki + p130wt
CaSki + p130mE7
CaSki + p130PM22
CaSki + p130PM22/mE7
p130
B-actin

Figure 3.11

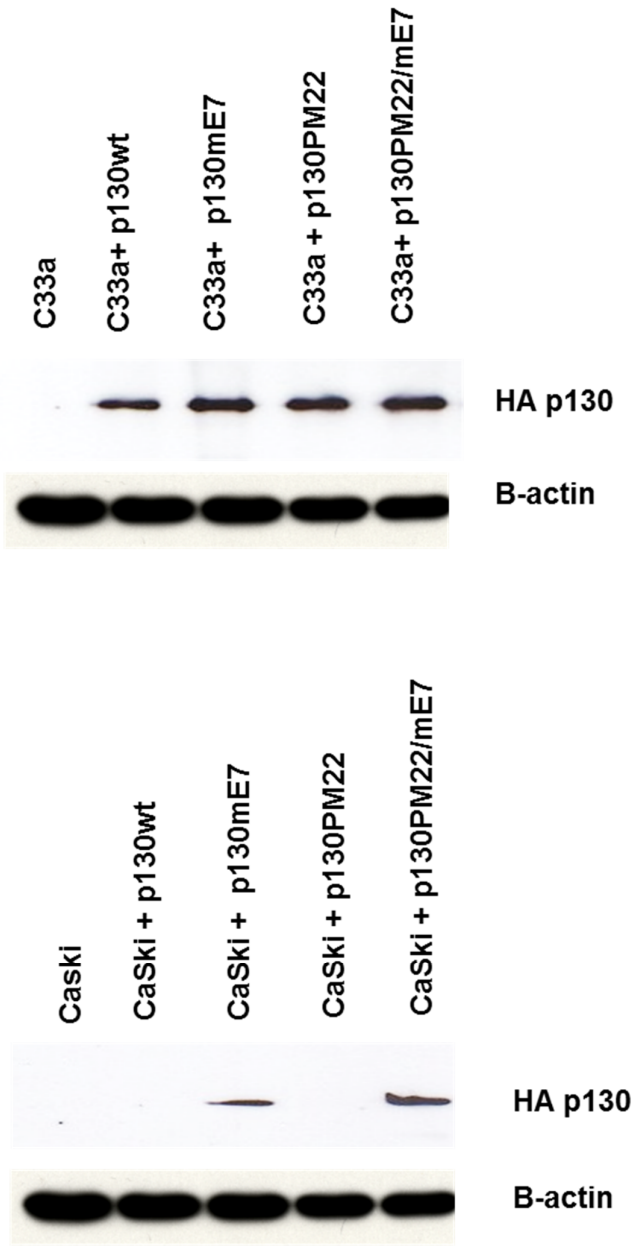
C33a
C33a+ p130wt
C33a+ p130mE7
C33a + p130PM22
C33a+ p130PM22/mE7
HA p130
B-actin
Caski
CaSki + p130wt
CaSki + p130mE7
CaSki + p130PM22
CaSki + p130PM22/mE7
HA p130
B-actin

Figure 3.11

anticipated from the expression levels of these proteins (Figure 3.12), the results showed that p130mE7 and p130PM22/mE7 were reformed into p130/DREAM complexes (Figure 3.12), whereas no p130/DREAM complexes were detected on this blot with the p130 wt or p130PM22 mutant. These results showed that mutation of the B pocket in p130mE7 and p130PM22/mE7 did not affect interactions with DREAM, whereas retention of E7-binding capability in p130wt and p130PM22 prevented their formation into DREAM complexes in CaSki cells. Unexpectedly, none of the Ha-tagged p130 proteins could be detected in DREAM complexes using the p130 antibody on western blots (Figure 3.12), again suggesting they were expressed at relatively low levels.

To assess whether transfection with wt p130 or any of the mutants had effects on the cell cycle in CaSki cells, transfected cells were harvested, stained with propidium iodide and analysed by flow cytometry. The mutants p130mE7 and p130PM22/mE7 were both able to arrest cells at G1, with 81% and 85.4% at this stage, respectively, compared to 56% G1 cells in control cells transfected with the empty vector . In contrast, neither p130wt nor p130PM22 had any effect on the cell cycle, with 55.7% and 55% at G1, respectively. These results reflected the ability of p130mE7 and p130PM22/mE7 to form DREAM complexes (Figure 3.13), and demonstrated that the levels of complex formation achieved with these mutants was sufficient to cause cell cycle arrest. It is notable that p130mE7 was as efficient as the p130PM22/mE7 double mutant in this cell cycle arrest assay, suggesting that direct interaction of 16E7 with p130 through its LXCXE motif is the key determinant in promoting the cell cycle in CaSki cells.

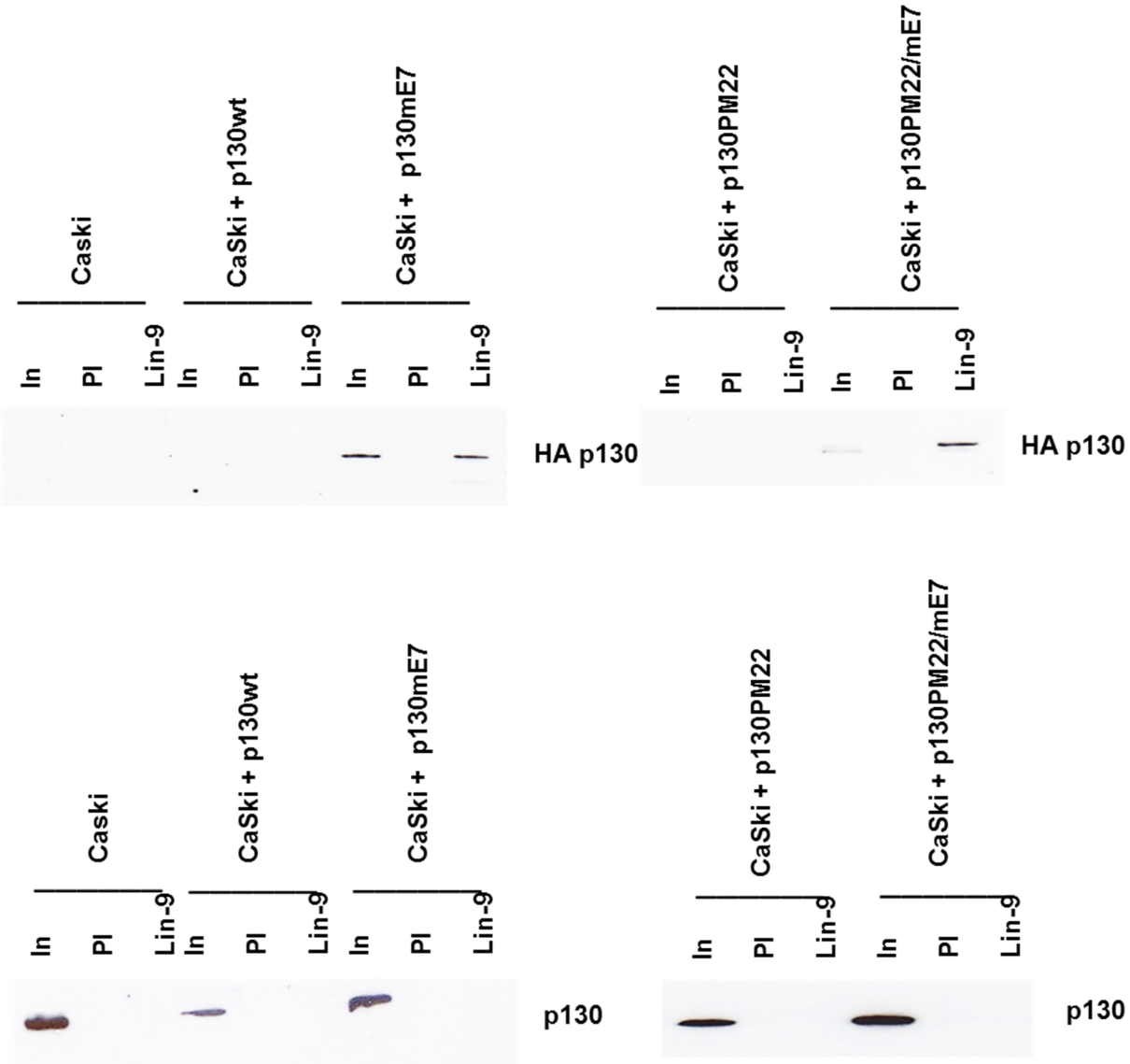

Figure 3.12: Identification of DREAM complex formation in CaSki cells transfected with p130 wt and the mutants p130mE7, p130PM22 and p130PM22/mE7. Nuclear lysates from untransduced CaSki cells (CaSki) or CaSki cells transfected with pMSCV puro constructed with p130 wt, p130 mE7, p130PM22 and p130mE7/PM22 were immunoprecipitated with pre-immune serum (PI) or Lin-9 antibodies and blotted for p130 and HA antibodies. The input (In) control comprised of the lysates used for immunoprecipitation.

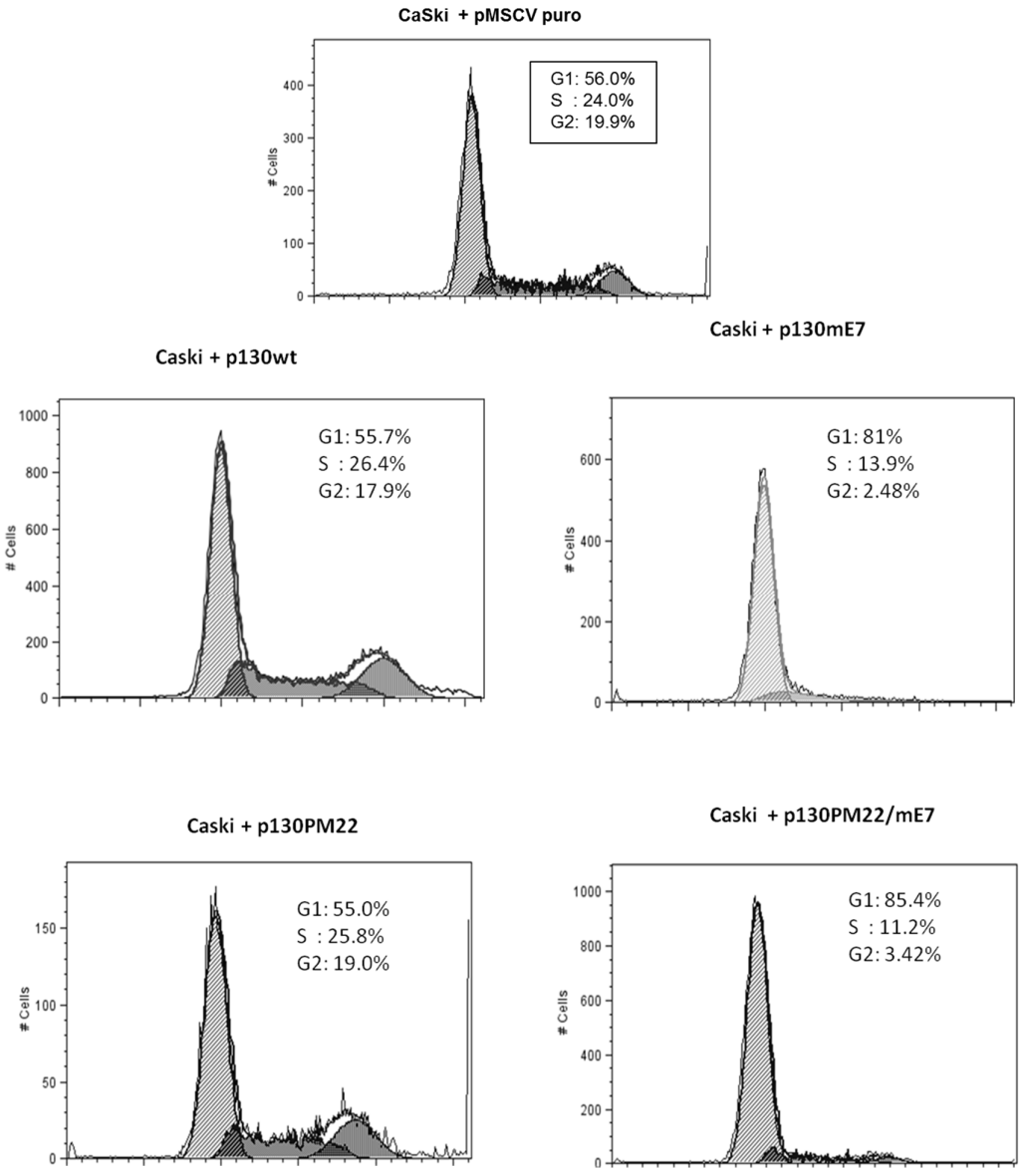

Figure 3.13: Flow cytometry (FACS) analysis in CaSki cells expressing various types p130 mutants. Flow cytometry of propidium iodide stained CaSki cells transfected with pMSCV puro constructed with p130 wt, p130mE7, p130PM22 and p130mE7/PM22 and pMSCV puro vector only as a control. The estimated percentages of cells in G1, S and G2/M phase are shown.

3.4.2 HPV16 E7 targets p130 predominantly through direct interactions via the LXCXE motif

To confirm that 16E7 targets p130 through its LXCXE motif, T98G cells were transfected with pMSCVpuro vectors encoding HA-tagged p130 wt, p130mE7, p130PM22 and p130PM22/mE7 together with 16E7. First, it was established that the p130 proteins were expressed equally and that expression of p130 had no effect upon 16E7 expression. Transfected cell lysates were collected, subjected to SDS-PAGE, western blotted onto PVDF membrane and the blot were then probed with HA antibodies. The resultant western blot (Figure 3.14) showed expression of 16E7 with only minor variation. The p130 wt and mutants were also consistently expressed in T98G cells (Figure 3.14).

It was then investigated what effect co-expression of 16E7 would have on the co-transfected p130 proteins. Whereas, co-expression with 16E7 had no significant impact on expression of p130mE7 or p130PM22/mE7 (Figure 3.14), it resulted in the virtual elimination of p130 wt and p130PM22 expression. The loss of p130 wt and p130PM22 expression in this experiment indicated that binding to 16E7 through the LXCXE motif resulted in proteasomal degradation, whereby the p130 proteins are degraded by the ubiquitin-proteasome pathway (Glickman and Ciechanover., 2002). HPV16 E7 and p130 both interact with and are ubiquitilated by SCF^{Skp2} complex (Oh et al., 2004; Tedesco et al., 2002).

As anticipated, formation of the DREAM complex with p130wt and p130PM22 was significantly disrupted by 16E7, whereas this complex was abundantly expressed with p130mE7 and p130PM22/mE7. Consistent with these results, analysis of T98G cell cycle status showed a profound G1 arrest when p130mE7 and p130mE7/PM22 were cotransfected with 16E7, with 87.5% and 82.5% of cells in G1, respectively,

whereas 16E7 co-transfection abolished the ability of p130wt and p130PM22 to cause G1 arrest (64% and 68.1% of cells in G1) (Figure 3.15).

Figure 3.14 :Ectopic expression of HPV16E7 with various types of p130 mutants in T98G cell lines (a) 20 μg of each pMSCVpuro-16E7-HA and co-transfected with each type of p130mutants construct and the pMSCVpuro vector control were calcium phosphate transfected for transient expression in T98G cells. Transfected cells were puromycin selected and nuclear lysates were harvested 48 hours post transfection. Nuclear lysates were immunoprecipitated with HA antibody, separated on a 15% SDS-PAGE gel and western blotted onto a PVDF membrane. 16E7 proteins were detected using HA antibody. (b) Nuclear lysates from T98G cells transfected with pMSCV puro constructed with 16E7HA or p130 wt, p130 mE7, p130PM2, p130mE7/PM22 and a combination of 16E7 with each of the p130s. Transfected cells were puromycin selected and nuclear lysates were harvested 48 hours post transfection. Nuclear lysates were separated on a 10% SDS-PAGE gel and western blotted onto a nitrocellulose membrane. HA p130 antibody was detected on western blots.

(c) Detection of ectopically expressed p130 in immunoprecipitates of T98G cells transfected with pMSCV puro constructed with p130 wt, p130mE7, p130PM22, p130mE7/PM22 and a combination of 16E7 with each of the p130 constructs. Pre-immune serum (PI) and Lin-9 antibodies were used for immunoprecipitation and HA p130 was detected on western blots.

a)

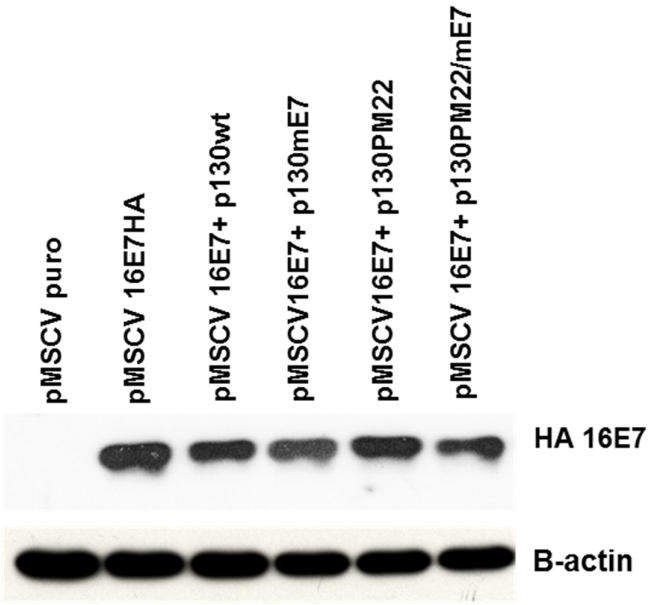

b)

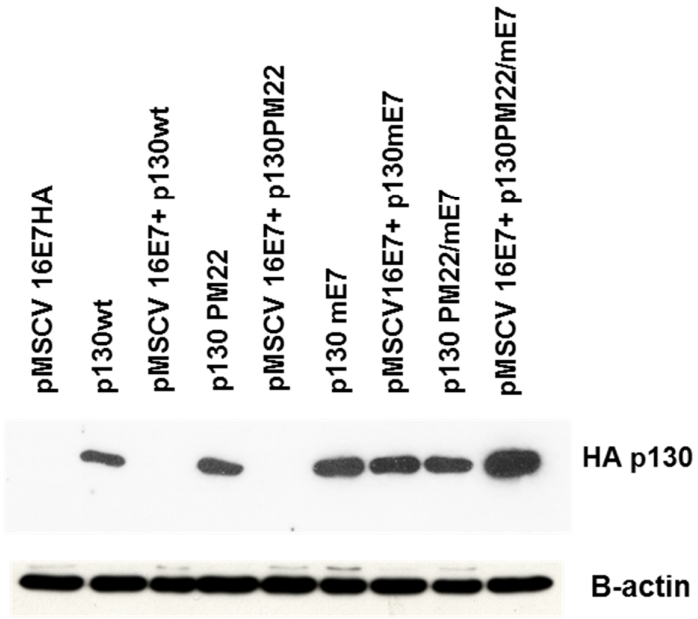

Figure 3.14

c)

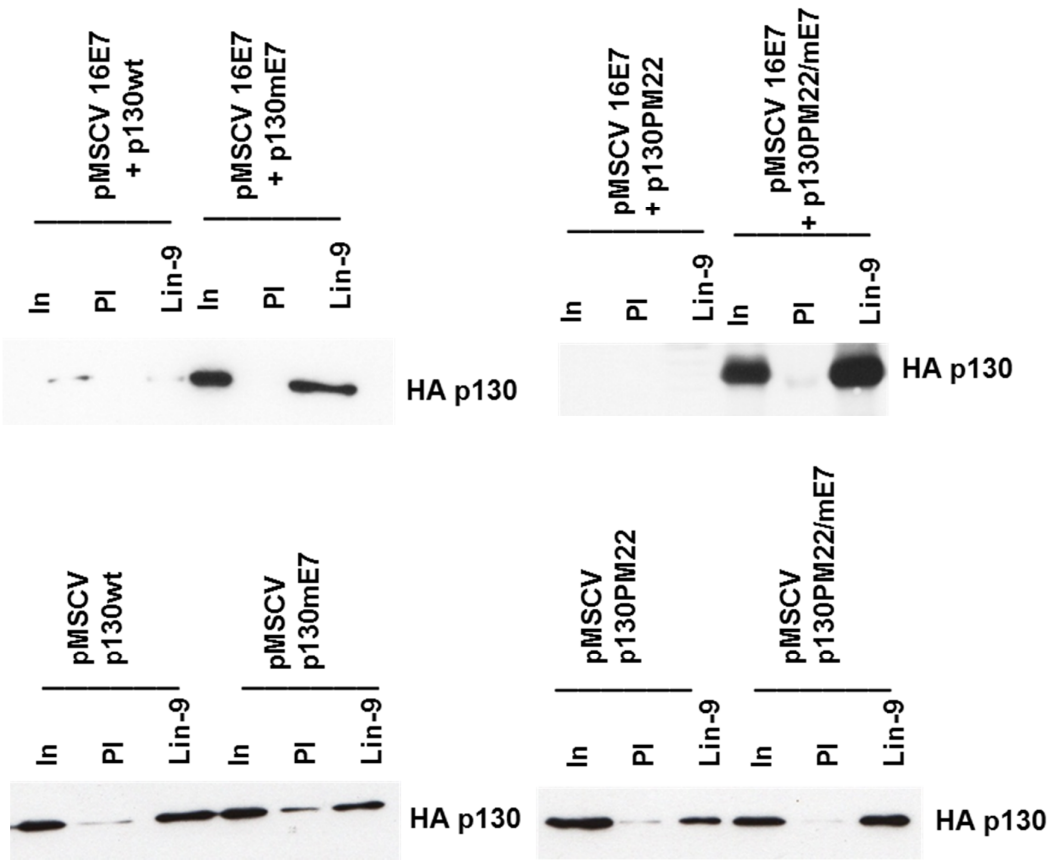
pMSCV 16E7 + p130wt
pMSCV 16E7 + p130mE7
pMSCV 16E7 + p130PM22
pMSCV 16E7 + p130PM22/mE7
In
PI
Lin-9
HA p130
pMSCV p130wt
pMSCV p130mE7
pMSCV p130PM22
pMSCV p130PM22/mE7

Figure 3.14

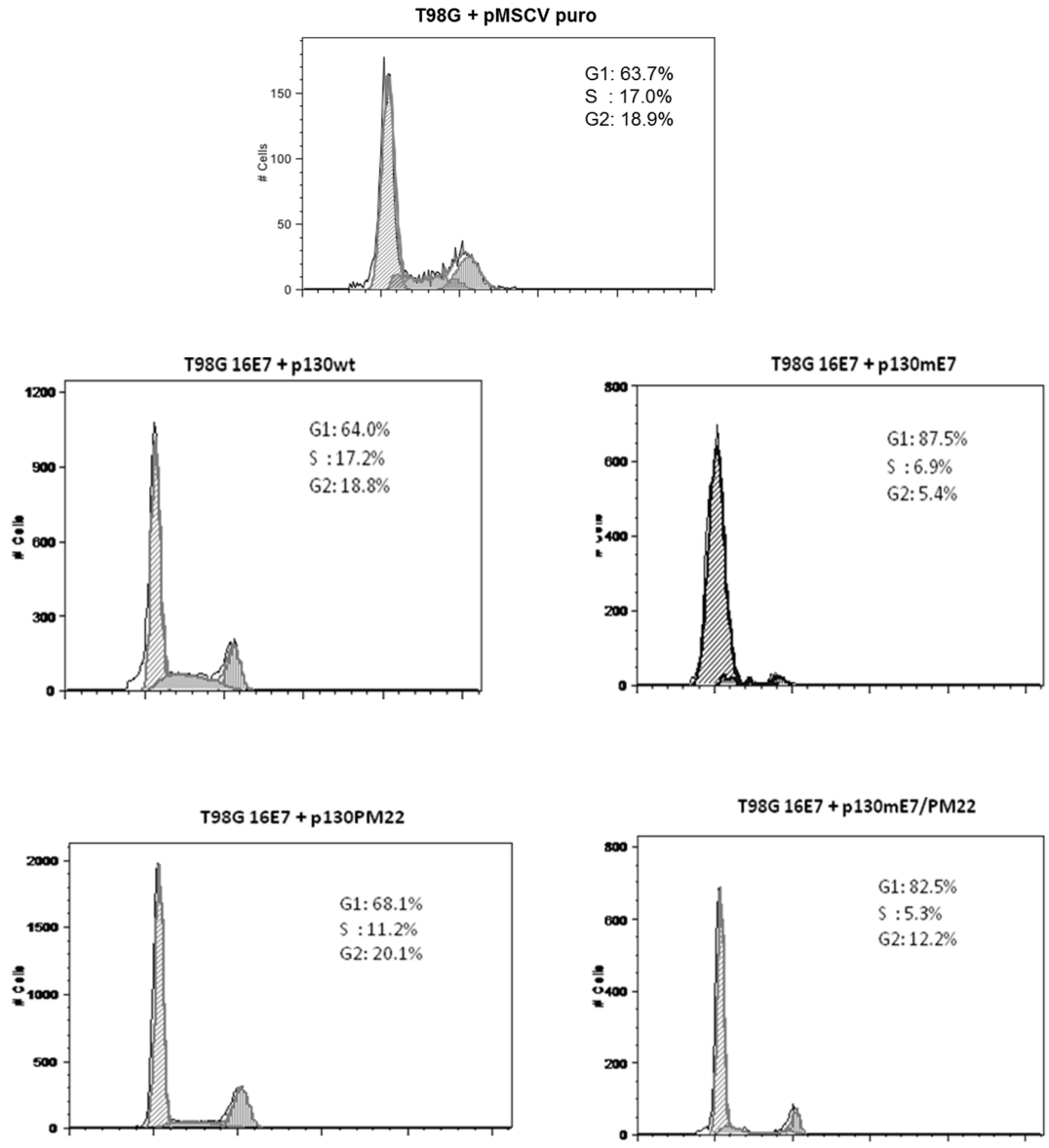

Figure 3.15: Flow cytometry (FACS) analysis of T98G expressing HPV 16E7 and various types of p130 mutants. Flow cytometry of propidium iodide-stained T98G cells transfected with pMSCV puro constructed with p130wt, p130mE7, p130PM22, p130mE7/PM22 together with 16E7HA. The T98G cells transfected with pMSCV puro only was used as a control. The estimated percentages of cells in G1, S, and G2/M phase are shown.

3.4.3 HPV 48E7 disrupts p130/DREAM via CDK2 phosphorylation

High risk and low risk HPV E7 proteins bind pRB family members via their LXCXE motif (Dyson et al., 1989). *In vitro* and *in vivo* studies revealed that HPV 16E7, as compared to HPV 6E7, has a greater affinity for pRB, p107 and p130 (Ciccolini et al., 1994; Gage et al., 1990). Casein kinase-II-mediated phosphorylation of high risk and low risk HPV E7 is necessary for effective binding to and destabilization of p130 (Genovese et al., 2008).

Pearce J., 2007; Ph.D thesis has shown that the cutaneous HPV 48E7 protein was competent to bind to the cdk inhibitor (Cdki), p21 *in vitro*. It is known that p21 together with p27 are involved in E2F/pocket protein-cyclin E/A-CDK2 pathways in G1 and S phase. By binding to p21, HPV 48E7 will abrogate its inhibition of cyclin/CDK activity and therefore prevent the association of p130 with E2F. This might lead to degradation of p130 and the disruption of p130/DREAM complex by 48E7.

Therefore, we wished to explore whether 48E7 disrupts p130/DREAM complex by binding towards p130 or via CDK inhibitor. The T98G human glioma cell line was used to express 48E7 and the HA-tagged wt and mutant p130 proteins used in the previous experiments. T98G cells were transfected with pMSCVpuro 48E7 as well as pMSCVpuro p130 wt, p130mE7, p130PM22 and p130PM22/mE7. The untransfected cells were eliminated by puromycin selection. To test whether expression of the 48E7 proteins was affected by co-expression with the p130, 100µg of cell lysates were run on an SDS-PAGE gel, western blotted and probed with HA antibody (Figure 3.16). Comparable levels of 48E7 were observed in each instance. To determine the effect of 48E7 against p130 wt and mutants, the pMSCVpuro vector encoding the p130 proteins were infected with either a vector control or pMSCVpuro 48E7.

Figure 3.16: Expression of HPV48E7 with various types of p130 mutants in T98G cell lines. (a) 20 μg of each pMSCVpuro-48E7-HA and co-transfected with each type of p130mutants construct and the pMSCVpuro vector control were calcium phosphate transfected for transient expression in T98G cells. Transfected cells were puromycin selected and nuclear lysates were harvested 48 hours post transfection. Nuclear lysates were immunoprecipitated with HA antibody, separated on a 15% SDS-PAGE gel and western blotted onto a PVDF membrane. 48E7 proteins were detected using HA antibody. (b) Nuclear lysates from T98G cells transfected with pMSCV puro constructed with 48E7HA or p130 wt, p130 mE7, p130PM2, p130mE7/PM22 and a combination of 48E7 with each of the p130s. Transfected cells were puromycin selected and nuclear lysates were harvested 48 hours post transfection. Nuclear lysates were separated on a 10% SDS-PAGE gel and western blotted onto a nitrocellulose membrane. HA p130 antibody was detected on western blots.

(c) Detection of ectopically expressed p130 in immunoprecipitates of T98G cells transfected with pMSCV puro constructed with p130 wt, p130mE7, p130PM22, p130mE7/PM22 and a combination of 48E7 with each of the p130 constructs. Pre-immune serum (PI) and Lin-9 antibodies were used for immunoprecipitation and HA p130 was detected on western blots.

a)

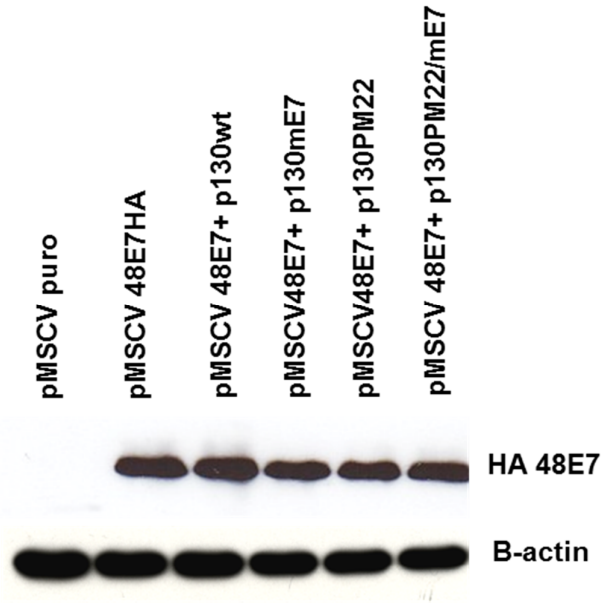

b)

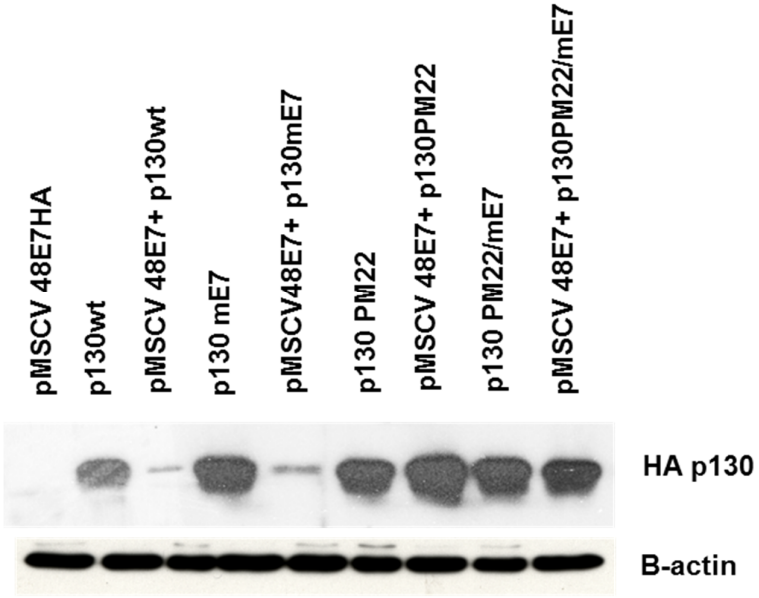

Figure 3.16

c)

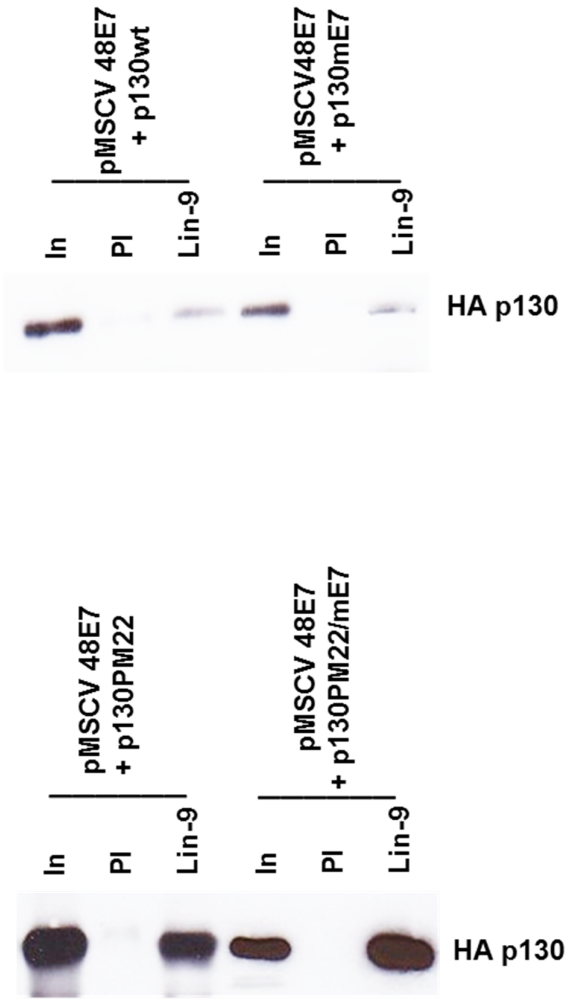
pMSCV 48E7
+ p130wt
pMSCV48E7
+ p130mE7
In
PI
Lin-9
In
PI
Lin-9
HA p130
pMSCV 48E7
+ p130PM22
pMSCV 48E7
+ p130PM22/mE7
In
PI
Lin-9
In
PI
Lin-9
HA p130

Figure 3.16

The transfected cell lysates were run on SDS-PAGE, immunoblotted and probed against HA= antibody. As shown in figure 3.16, both p130wt and p130mE7 were degraded when 48E7 was co-expressed, whereas p130PM22 and p130PM22/mE7 were unaffected by 48E7. These findings are consistent with the *in vitro* experiment by Pearce J.,2007 indicating 48E7 has extremely low affinity to bind to p130. Twenty- two phosphorylation sites in both p130 phospho-site mutant (p130PM22 and p130PM22/mE7) have been replaced with alanine instead of serine and threonine. Cyclin dependent kinases (CDKs) always phosphorylate serine and threonine by the proline sites of p130. Therefore the blot from figure 3.16 has proven that 48E7 disrupts p130 expression through CDK phosphorylation. It is most probable that this activity reflects binding of 48E7 to the CDK2 inhibitor p21, which inevitably abrogates the inhibition of cyclin/CDK activity and prevents the assembly of the p130/DREAM complex.

Immunoprecipitation with Lin-9 antibody demonstrated that the p130/DREAM complex was significantly reduced when p130wt and p130mE7 were co-expressed with 48E7, compared to formation of this complex with p130PM22 or p130PM22/mE7 (Figure 3.16). To determine what impact this would have the ability of the various p130 proteins to arrest the T98G cell cycle, the transfected cells were harvested and subjected to propidium iodide staining. Flow cytometry analysis shown that cells were arrested at G1 phase for both p130PM22 and p130PM22/mE7 were co-expressed with 48E7 (80.2% and 89.9% cells in G1, respectively), whereas cells expressing p130wt or p130mE7 were able to escape G1 arrest in the presence of 48E7 (Figure 3.17).

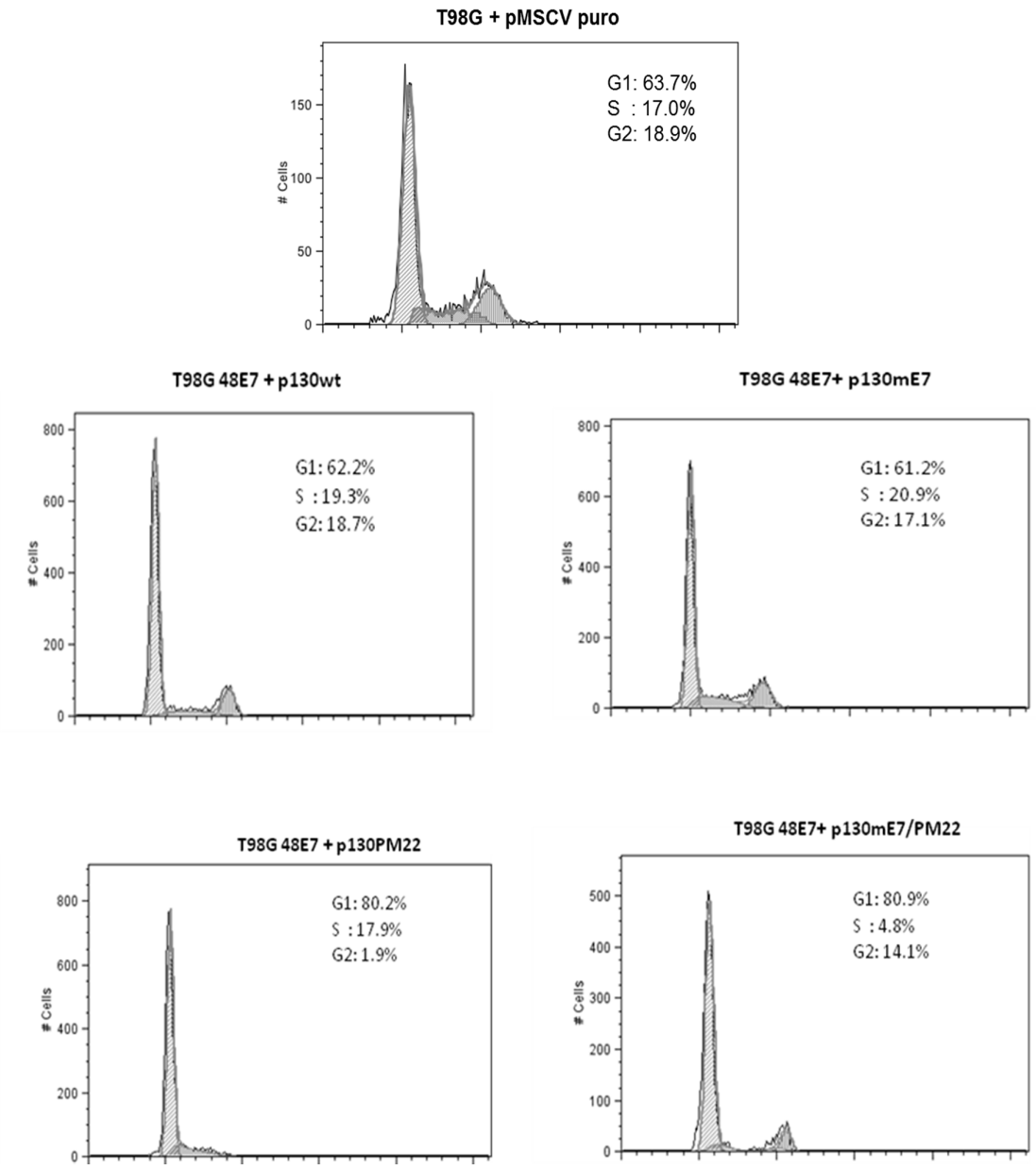

Figure 3.17: Flow cytometry (FACS) analysis of T98G expressing HPV 48E7 together with various type of p130 mutants. Flow cytometry of propidium iodide-stained T98G cells transfected with pMSCV puro constructed with p130wt, p130mE7, p130PM22, p130mE7/PM22 together with 48E7HA. The T98G cells transfected with pMSCV puro only was used as a control. The estimated percentages of cells in G1, S, and G2/M phase are shown.

3.5 Function of the B-myb/DREAM complex in Caski cells.

Recently, (Knight A.S *et al*., 2009) have shown that the B-myb/DREAM complex is required for transit through mitosis in embryonal stem cells which lack pocket protein/DREAM complexes. They also had found a pronounced defect in completing mitosis by targeting one of the DREAM complex members (Lin-54). Therefore with this understanding, we wished to investigate whether B-myb/DREAM has a similar function in HPV16-transformed cells, which also have deficient pocket protein/DREAM complexes. This question is significant, because previous experiments (Figure 3.2) showed increased B-Myb/DREAM expression in CaSki and SiHa cells, at least when compared to the T98G cell control, suggesting that disruption of the repressive p130/DREAM complex by 16E7 promotes the formation of the transcriptionally active B-Myb/DREAM complex, which could then have a positive impact on cell cycling.

Real-time PCR was carried out in order to investigate the silencing level of Lin-54 at the mRNA level. Three different cell lines were used in this experiment, T98G, SiHa and Caski. As shown in Figure 3.18a and b, the transduction of T98G and SiHa cells with Lin-54 shRNA resulted in a significant decrease of Lin-54 mRNA by 98.5% and 97.7%, respectively. However, only 58% of Lin-54 mRNA was reduced in Caski cells as shown in Figure 3.18c. As the transduced cells were puromycin selected, the inefficient knockdown of Lin-54 in Caski cells should not reflect low transduction. There are several spliced forms of Lin-54 mRNA and it is possible that qPCR detected forms which were not targeted by Lin-54-1 shRNA. To further determine whether Lin-54 knock-down affected B-Myb/DREAM complex association in Caski cells, co-immunoprecipitation with three of the DREAM complexes constituents (Lin-9, Lin-54 and B-myb) was carried out. The blot was probed against B-myb,

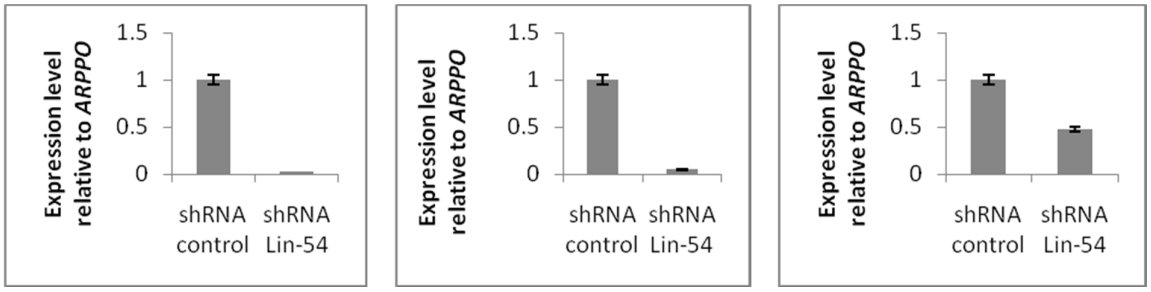

d)

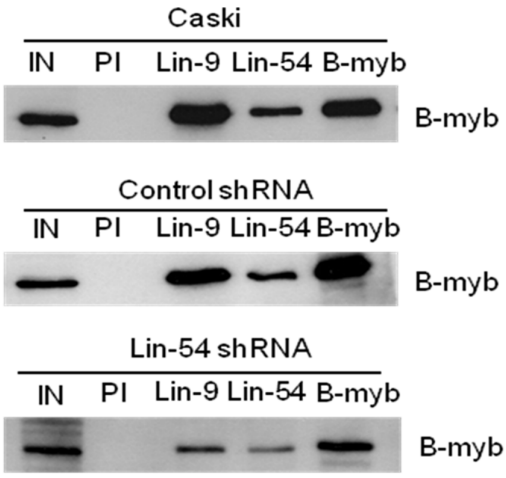

Figure 3.18: Depletion of Lin-54 in T98G, SiHa and Caski cells. Quantitative RT-PCR analyses of Lin-54 expression in Lin-54-depleted cells (a) T98G (b) SiHa (c) Caski relative to control cells. Expression was normalized to ribosomal *ARP PO*. (d) Nuclear lysates from Caski, Caski transduced with scrambled shRNA (control) and Caski transduced with Lin-54 shRNA cells were immunoprecipitated with preimmune Lin-9 rabbit serum (PI), Lin-9, Lin-54 and B-myb antibodies and western blotted for B-myb. The input control (IN) comprised 10% of the lysates used in immunoprecipitation.

as B-myb is highly expressed in Caski cells. As demonstrated in figure 3.18 d, the association of B-myb with both Lin-54 and Lin-9 was equally decreased by depleting Lin-54 in Caski cells. This suggest that Lin-54 is necessary for the stability of the DREAM complex or its association with B-myb.

To determine the effects of Lin-54 suppression on cell cycle progression, FACS analyses were performed. In this experiment, T98G, SiHa and Caski cells were employed and the transduced cells were harvested 48 hours post-transduction. These cells were stained with propidium iodide and analyzed with flow cytometry. The results (Figure 3.19) demonstrated that Lin-54 depletion caused an increased proportion of G2/M cells in T98G and SiHa cells, with 32.3% and 19.3% with 4n content when compared to control 17.9% and 10.8%, respectively. Depletion of Lin-54 in Caski cells also showed accumulation in G2/M phase with 21.2% with 4n content compared to control 15.9%.

To investigate how critical the B-myb/DREAM complex function is in Caski cells, we further determined the effect of Lin-54 knockdown on mRNA levels of certain S/G2 genes, such as cyclin B, aurora kinase A and Polo-like kinase-1. Theoretically, since depleting Lin-54 in Caski cells resulted in B-myb/DREAM complexes being down-regulated, S/G2 gene expression may be reduced in their expression. However, the expression level of these genes was marginally increased in Caski cells when compared to the control shRNA cells (Figure 3.20). Whereas Lin54 depletion resulted in expression of all three S/G2 genes being decreased in T98G cells, in SiHa cells only Aurora kinase A gene was decreased.

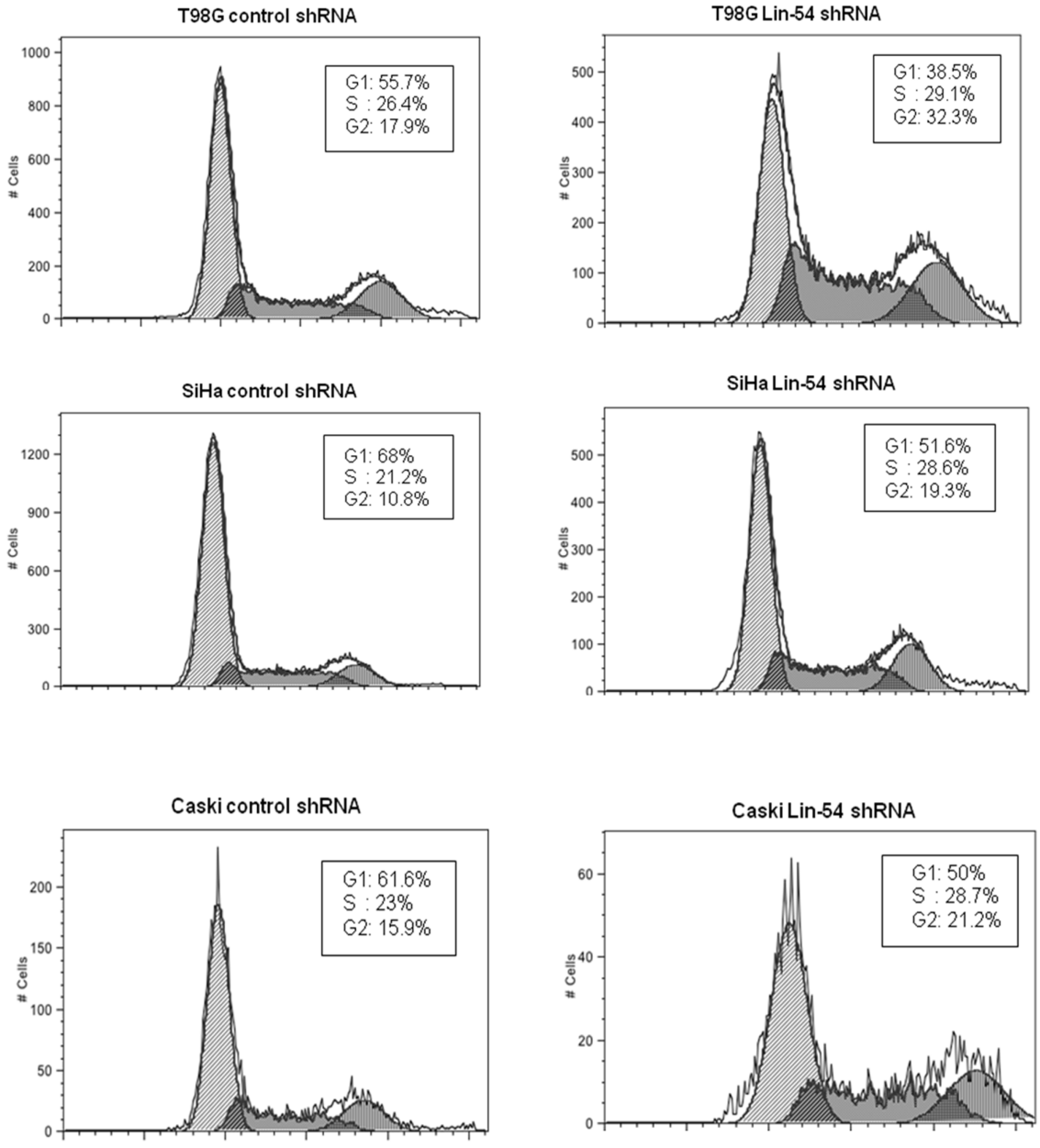

Figure 3.19: Effects on cycle progression by depleting Lin-54 in T98G, SiHa and Caski cells. Cells were stained with propidium iodide (PI) to count the DNA content.

a)

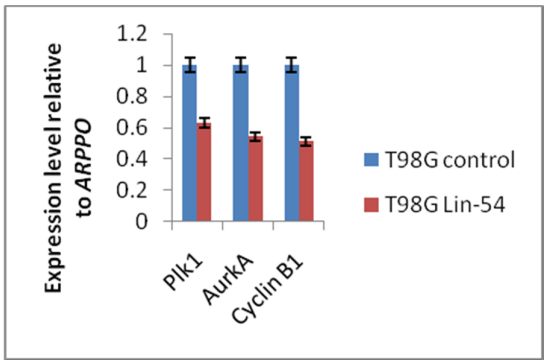

b)

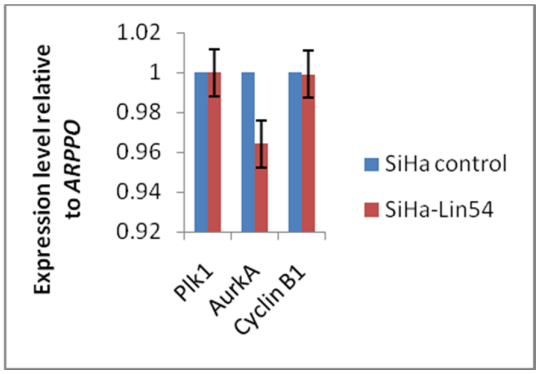

c)

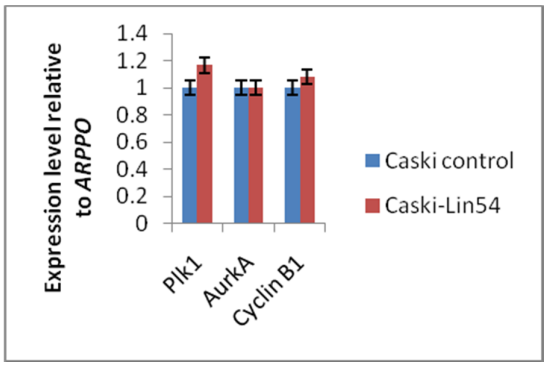

Figure 3.20: Analysis of G2/M genes suppression in Lin-54-depleted cells (a) T98G, (b) SiHa and (c) Caski. Quantitative RT-PCR analysis of B-myb target genes in Lin-54-depleted cells relative to control cells (scrambled shRNA). Expression was normalized to *ARP PO*.

CaSki cells lack of pocket proteins/DREAM complexes, and the results demonstrate that in this context B-myb/DREAM complexes are not critical in regulating these S/G2 genes.

In addition, to further test the B-myb/DREAM complex function, we further knock down the other main components of core DREAM complex, which is Lin-9. We showed that the results were consistent with Lin-54 depletion in CaSki cells as shown in Figure 3.21, the mRNA levels of cyclin B, aurora kinase A and polo-like kinase-1 were increased when compared to control shRNA. Flow cytometry analysis showed that Lin-9 Caski-depleted cells is increased by 2% compared to control cells 16.6%. This results showed that B-myb/DREAM complex is not critical in regulating CaSki cells.

However, these results were further confirmed by depleting the B-myb itself in CaSki cells. As anticipated, the results in Figure 3.22 showed the same pattern of cell cycle and mRNA level for S/G2 genes when compared to Lin-54 and Lin-9 depleted cells. Therefore, we can conclude that B-myb /DREAM complex is not critical in cell cycle regulation in CaSki cells.

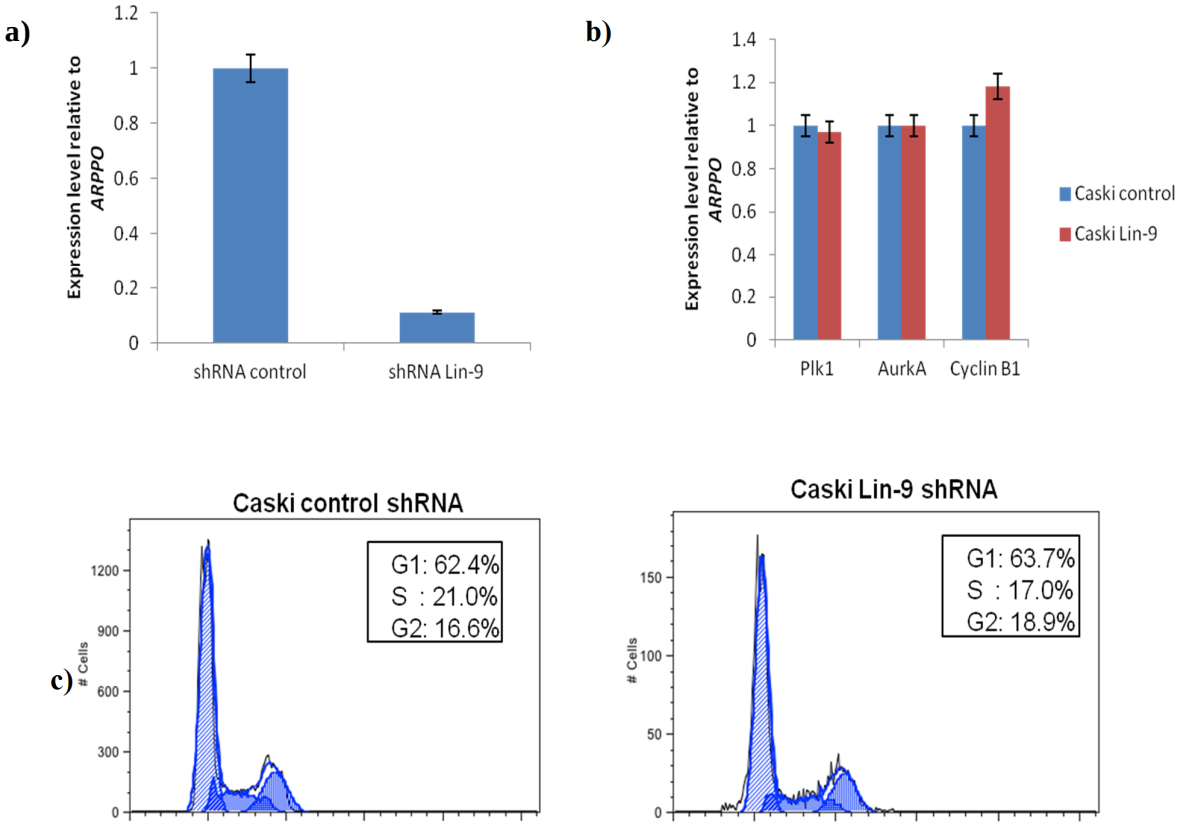

Figure 3.21: Depletion of Lin-9 in CaSki cells. (a) Quantitative RT-PCR analysis of Lin-9 expression in Lin-9 depleted cells. Expression was normalised to ribosomal ARP PO. (b) Quantitative RT-PCR analysis of Lin-9 target genes in Lin-9 depleted celles relative to control cells (scrambled shRNA) and expression was normalised to ARPPO. (c) Flow cytometry of propidium iodide-stained Lin-9 depleted CaSki cells. The estimated percentages of cells in G1, S and G2/M phases are shown.

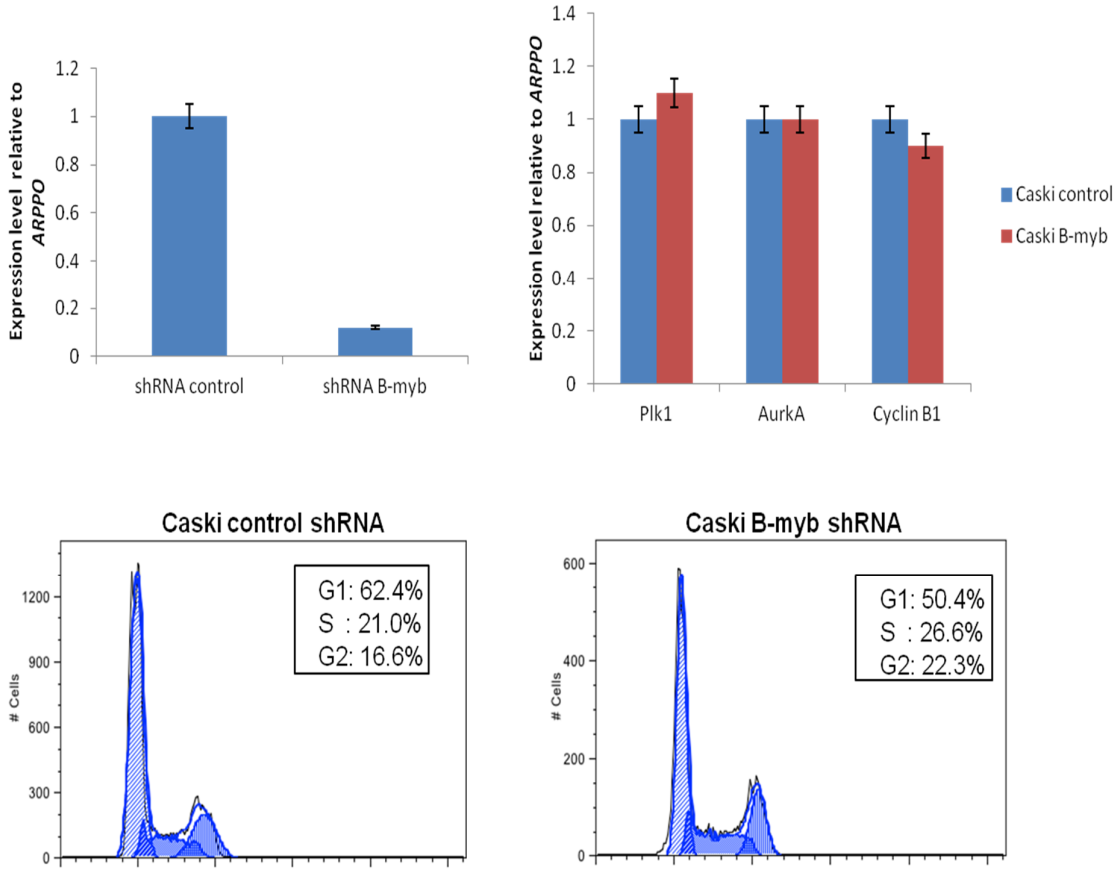

Figure 3.22: Depletion of B-myb in CaSki cells. (a) Quantitative RT-PCR analysis of B-myb expression in B-myb depleted cells. Expression was normalised to ribosomal ARP PO. (b) Quantitative RT-PCR analysis of B-myb target genes in Lin-9 depleted celles relative to control cells (scrambled shRNA) and expression was normalised to ARPPO. (c) Flow cytometry of propidium iodide-stained B-myb depleted CaSki cells. The estimated percentages of cells in G1, S and G2/M phases are shown.